University of New Mexico
UNM Digital Repository

7-1-2016

Investigation of Interfacial Interaction of Manganese Oxides with Organic Micropollutants

Mohamed Nabil Shaikh

Follow this and additional works at: https://digitalrepository.unm.edu/ce_etds

Recommended Citation

Mohamed Nabil Shaikh

Candidate

Civil Engineering

Department

This thesis is approved, and it is acceptable in quality and form for publication:

Approved by the Thesis Committee:

Dr. José M. Cerrato, Chairperson

Dr. Abdul Mehdi Ali

Dr. Kerry Howe

INVESTIGATION OF INTERFACIAL INTERACTION OF MANGANESE OXIDES WITH ORGANIC MICROPOLLUTANTS

by

MOHAMED NABIL SHAIKH

B. E. IN CHEMICAL ENGINEERING

THESIS

Submitted in Partial Fulfillment of the
Requirements for the Degree of

Masters of Science
Civil Engineering

The University of New Mexico
Albuquerque, New Mexico

July 2016

iii

Acknowledgements

I would like to convey my appreciation to Dr. José M. Cerrato, my advisor and committee chairperson, for his mentorship and guidance in my research. His enthusiasm and passion has made me appreciate academia and develop my scientific attitude. His meticulous supervision and direction has helped me in completion of this thesis and his education will guide me to successfully navigate my career. I want to express my gratitude to Dr. Cerrato and University of New Mexico School of Engineering Startup Fund for providing funding towards my education and research.

I would also thank Dr. Abdul Mehdi Ali for his immense knowledge and experience in the scientific field, especially analytical chemistry. His support and guidance has embedded the values of proper experimental and analytical procedures in me. I would like to thank Dr. Kerry Howe for his invaluable teaching in the fundamentals and principles of water treatment. I would thank my committee Dr. Cerrato, Dr. Mehdi and Dr. Howe, again for their patience, understanding and guidance through my research and towards my graduation.

I would also thank Dr. Huichun Zhang for her incredible support, input and guidance in this study and I appreciate the help provided by her students, Saru Taujale and Kowsalya Rasamani with batch experiments and analysis.

Finally, I must thank my father Ismail, mother Khursheed, sisters Moza and Nahid, and my wife Sadia for their boundless love, patience and support for my success and ambitions. Without them, I would not be where I am today.

INVESTIGATION OF INTERFACIAL INTERACTION OF MANGANESE OXIDES WITH ORGANIC MICROPOLLUTANTS

by

Mohamed Nabil Shaikh

B. E. in Chemical Engineering, 2012

M.S. in Civil Engineering, 2016

ABSTRACT

Water reuse has become a necessary practice in arid and semi-arid regions like the Southwestern USA. However, a new generation of emerging organic micropollutants has been increasingly scrutinized in water sources. The aim of this study is to determine the changes in chemical composition occurring on the $MnO_x(s)$ surface after reaction with organic micropollutants using X-ray Photoelectron spectroscopy (XPS), Raman spectroscopy and solution chemistry analyses. Laboratory batch experiments were conducted to assess the reactivity of $MnO_x(s)$ with aniline, triclosan, phenol and bisphenol A. Analyses of XPS high resolution scans through the determination of the shape and position of Mn 3p spectra and Mn 3s multiplet splitting suggest that Mn(III) and Mn(II) increase in the surface of $MnO_x(s)$ reacted with organics, indicating that organic oxidation causes the reduction of $MnO_x(s)$. Impurities on $MnO_x(s)$ surface (eg. other metal oxides) decrease the micropollutant removal efficiency. After the rapid initial oxidation of micropollutants, the availability of surface sites was found to be a major factor influencing the long-term reaction rates. Aniline and Bisphenol A were still detectable after reaction completion due to surface sites being irreversibly occupied by reaction products or impurities. The results from this research are applicable for the mechanistic comprehension of interactions between $MnO_x(s)$ and organic micropollutants, which is necessary for understanding the $MnO_x(s)$-micropollutant geochemical processes and development of water treatment technologies that use $MnO_x(s)$ to remove organic micropollutants.

TABLE OF CONTENTS

List of Figures

List of Tables

Chapter 1

Introduction

The thesis has been divided into 3 chapters and 2 appendixes. Chapter 2 is a summary on the scientific knowledge on the topic, including a background on manganese and organic micropollutants, ending with a review of research gaps and limitations in the proposed field of study. Chapter 3 is the main body of work of the thesis, formatted as a research paper which will be submitted to the peer-reviewed journal *Environmental, Science & Technology*. The main topic covered in Chapter 3 relates to the investigation of interfacial chemistry reactions of $MnO_x(s)$ with triclosan, aniline, and phenol. The objective of the study presented in Chapter 3 was to investigate the reaction of manganese oxide ($MnO_x(s)$) with phenol, aniline and triclosan using X-ray photoelectron spectroscopy and Raman spectroscopy. Chapter 3 includes a discussion of the observed spectroscopy and aqueous chemistry results, and provides potential mechanistic explanations and environmental implications of this study. The Appendix A contains supplementary data obtained for the study presented in Chapter 3. Appendix B provides a preliminary report of an investigation of the effect of surface area and metal impurities on the effective application of $MnO_x(s)$ for the removal of bisphenol A (BPA). The work presented in Appendix B will serve as a foundation for the work that I will be conducting in my Ph.D. studies which I will continue to pursue at the University of New Mexico.

1

Chapter 2

Background and Literature Review

1. Background and Significance:

The occurrence of organic micropollutants is an emerging concern in natural and engineered water systems.[1,2] The major source of these contaminants are pharmaceutical and personal care products (PPCPs) which are discharged in the environment through waste water and landfill leachate.[3,4] These micropollutants have been found to be eco-toxic and most are classified as endocrine disrupting compounds (EDCs).[5,6] Their presence in surface water has caused negative impacts on aquatic ecosystems such as gender confusion, olfactory disruption leading to loss of homing behavior, mutation of reproductive organs and retarded growth.[7–9] Thus, the development of effective water treatment technologies that target removal of organic micropollutants is necessary.

The removal of organic micro-pollutants in wastewater and water reuse treatment facilities is challenging given that the micropollutants are present in trace concentrations and co-occur with high concentrations of dissolved organic matter. Current technologies used at water treatment facilities typically include physical process like coagulation, adsorption, filtration, and oxidative processes. For example, the removal of atrazine (a herbicide with strong endocrine disruption) in jar tests with coagulation and powdered activated carbon (PAC) sorption has been reported at a maximum of 73% at the end of 5 days (equilibrium).[10] However, water treatment facilities have a shorter residence time compared to this 5 day equilibrium. Effective removal of phenolic micropollutants has been accomplished by oxidation using chlorination or ozone,[11] although, many of the

2

micropollutants form oxidized by-products which could also be harmful.[2,12] Ozonation provides good removal for phenolic micropollutants,[13] but the formation of radicals is a concern due to potential carcinogenic effect [14,15] and byproducts such as bromate (BrO_3^-) in bromide containing water.[13,16] Ozonation is also nonselective with various micropollutants as a very small percent of OH radicals react with the target micropollutant.[14] Lack of disinfectant residual, fouling, and high initial and operational expenses is a significant disadvantage for ozonation.[3,15] Innovative technologies should be developed using cost-effective methods to remove these micropollutants.[1]

Manganese oxides (MnO_x) have been known to be excellent oxidants with ability to remove inorganics such as heavy metals from drinking water.[17] Manganese oxides are natural scavengers of metals in the environment due to their known redox reactivity and adsorptive capacity.[18] Due to this nature, MnO_x can be ubiquitously found in natural systems around the world and play a key role in biogeochemical processes.[19,20] Vast amount of research has been done with inorganic contaminant removal using MnO_x [17,21–24] and current literature shows evidence of MnO_x reactivity with many organic micro-pollutants specifically phenolic and aniline based compounds.[25–31] The following subsections will discuss in more detail different aspects of the mineralogy, biogeochemistry, occurrence, and application of MnO_x in natural and engineered environments.

2. Manganese in Nature

Manganese is one of the most ubiquitous metals in nature. It is the third most abundant transition metal. However manganese does not exist in nature as a free element;

3

it is usually associated with oxygen to form solid oxides, hydroxides or oxy-hydroxides. Manganese oxides (MnO_x) are one of the most abundant oxides found in soil and sediments. Manganese can exist in various oxidation states in nature (e.g. 0, +2, +3, +4, +6 and +7); oxidation states +2, +3 and +4 are the most significant in nature. Oxidation state +2 state is generally soluble in water; while oxidation state +4 is generally insoluble. Redox chemistry plays an important part in the dissolution and precipitation of manganese, with reducing environment favoring presence of the aqueous Mn(II) and oxic environment favoring Mn(IV) oxides. MnO_x usually associates itself to other materials such as organic matter,[32–34] iron oxides [32,35] and silica/sand particles (coated sand).[36–38] Hence it is common to find many forms of manganese in nature, some of which are described below.

2.1. Mineralogy of MnO_x

The different Mn oxidation states result in various forms of MnO_x(s) mineral phases. The elementary lattice unit of most MnO_x(s) minerals is edge sharing MnO_6 octahedron. The octahedral assemble together to form two groups of major crystal structures; (a) chain or tunnels, and (b) layer structures.[26,39] A chain is formed by multiple edge sharing MnO_6 octahedra, which can share corners with other chains resulting formation of tunnels. Layer MnO_x(s) are formed by stacking of sheets of edge sharing MnO_6 octahedra. Water molecules and cations can be accommodated in the interlayer region of the mineral structure.[21,40] The most common forms of MnO_x(s) and information about properties such as surface area and structure are illustrated in **Table 1**.

Pyrolusite is an abundant tunnel form of MnO_x(s), consisting of a framework of 1 x 1 MnO_6 octahedral tunnel structure which does not allow for other chemical species to

4

be present, resulting in a pure MnO_2 composition. Pyrolusite are usually referred to as β-MnO_2 and are found in hydrothermal deposits.[39] Todorokite is another common tunnel form of $MnO_x(s)$ mineral consisting of multiple MnO_6 octahedral triple chains to form a complex framework of tunnels.[41] The space in the cross section is usually occupied by a cation such as Co, Cu or Ni. Todorokites can be found as Mn coatings / dendrites on rocks and surfaces and in marine Mn nodules.[39,41]

Table 1. Properties of different $MnO_x(s)$ minerals

Mineral	Structure	Surface Area (m^2/g)	Notes
Pyrolusite	Tunnel (1x1)	7.5 [a]	Mostly pure MnO_2 with no associated cations
Todorokite	Tunnel (3x4 upto 3x9)	32.7 [a]	Mg, Co, Cu or Ni are associated cations
Triclinic Birnessite	Layered	39 [b]	Unstable at low pH, reverts to hexagonal structure like other birnessites
c disordered H^+ Birnessite	Layered	154 [b]	Similar to δ-MnO_2 but different order in layered structure and Mn(IV)/Mn(III) ratio
δ-MnO_2	Layered	128.3	Also known as vernadite, and a synthetic analog to biogenic MnO_x [b]

Surface Area determined by BET with N_2 gas adsorption
  a   Cited from Kim et. al. (2000) [21]
  b   Cited from Villalobos et. al (2003) [42]

Birnessite are the most common form of $MnO_x(s)$ mineral found in nature,[21,42,43] structurally consisting of multiple hexagonally symmetric sheets of MnO_6 octahedra stacked on each other, with cations and water molecules occupying the interlayers. Birnessites are poorly crystalline, have a good cation exchange capability and found as a major phase of $MnO_x(s)$ coatings in soils, dendrites varnishes and ocean nodules.[18,43] Different forms of birnessites have been discovered, studied and classified by interlayer spacing, major cation or preparation technique. The term delta Manganese oxide 'δ-MnO_2'

5

has been used to designate various analogous forms of synthetic Mn oxide phases such as birnessite[17,23,37] or vernadite[22,39]. A study by Friedl et al.[22] used EXAFS spectroscopy and suggested that vernadite can be considered as a c-disordered H^+ birnessite. However, the molar ratio of Mn(III) to Mn(IV) in vernadite is different from that in δ-MnO_2.[42] Studies[40,42–44] show that the closest synthetic analog to biogenic MnO_2 is vernadite (δ-MnO_2) with the same local molecular structure as randomly-stacked birnessite, but with smaller crystallite size along the c-direction. These similarities in structure weigh against adopting separate mineral names for vernadite and birnessite, instead the consensus is to use the unit cell symmetry as prefix to the current nomenclature.[42]

2.2. Biogeochemical Cycles of Mn

The strong $MnO_x(s)$ redox activity and high surface area make them an important part of the bio-geochemical cycle of many compounds, nutrients and contaminants. $MnO_x(s)$ are very good scavengers of metals in natural system due to redox or sorption, as seen by their exceptional ability to influence other elements even concentrations much higher than that of $MnO_x(s)$.[39] The mechanism of scavenging action is caused by negative charges (due to Mn(III) or Mn(II) defects on MnO_2) or vacant sites in the mineral lattice[44]. Metal ions and metallic species get sorbed onto the $MnO_x(s)$ either by inner/outer sphere complexes;[18,37] by translocation into the tunnels/interlayer regions;[45] or by incorporation of into the $MnO_x(s)$ structure by substitution for Mn or vacant sites within the mineral.[24,44] $MnO_x(s)$ plays an important role in scavenging of uranium and other transuranic elements. Studies [24,45,46] show that U(VI) had a strong affinity to bind with $MnO_x(s)$ preferentially over other minerals such as iron oxides. The strong Cu scavenging action of δ-$MnO_x(s)$ in

6

deep ocean/marine systems is not only due to surface complexation or occupation of the vacant sites, but due chelation to microbially generated ligands.[18] Similarly, As oxidation by MnOx(s) in the environment is significant since conversion of arsenite As(III) to arsenate As(V) causes decrease in As mobility and sorption onto $MnO_x(s)$ minerals.[47] $MnO_x(s)$ are the only confirmed natural oxidant of Cr(III) in the surface.[21,48] and control the formation of toxic hexavalent Cr(VI).[23] The significance of $MnO_x(s)$ in marine sediments towards nitrogen cycle has been demonstrated, with $MnO_x(s)$ driven conversion of organic N and NH_3 into N_2.[49] Reduction of nitrates to N_2 by dissolved Mn(II) species in anoxic conditions has also been observed, resulting formation of $MnO_x(s)$.[50]

The presence of Mn(III) solid phase has been demonstrated as an important part of Mn biogeochemical cycle.[35,51] A general consideration is that Mn(III) usually occurs as a short-lived intermediate and disproportionates into Mn(II) and Mn(IV). However, studies have shown that Mn(III) does exists in stable soluble forms in suboxic zones [20,35] or with organic complexes,[44,49,52] or in solid mineral phases (e.g., Mn_2O_3, MnOOH, among others).[51,53,54] The solid Mn(III) would affect the Fe(III) bioavailability and thus impact the biogeochemical cycling of major elements like C, N, and S.[51] Mn(IV) is considered to be the dominant Mn solid phase in natural systems, Mn(II) is soluble and found in low pH and anoxic conditions. The Mn(IV), Mn(III) and Mn(II) speciation reactions occurring in the environment and the associated standard reduction potential are illustrated in **Table 2**.

Microbial activity is an important mechanism in the cycling of $MnO_x(s)$ in nature. Microbes can conduct redox reactions of Mn by direct enzymatic activity or by indirect (dissimilatory) interactions. Manganese oxidizing microorganism rapidly accelerate the mineralization of Mn much faster than abiotic formation on a mineral surface or

7

homogenous oxidation in aqueous solutions.[26,44] Many Mn(II) oxidizing bacterial species have been identified in natural aqueous systems, divided into three distinct phylogenetic types; Proteobacteria (Gram positive, α, β, and γ), low Firmicutes, and high Actinobacteria.[42,44] There are two mechanism of bacterial oxidation of Mn(II); (a) directly by production of polysaccharides or proteins which catalyze the oxidation; (b) alternate mechanism is indirect oxidation by modifying the local redox/pH conditions or by releasing products that will cause chemical oxidation of Mn(II). [44]

Table 2. MnO_x geochemical Mn speciation reactions with the Standard Reduction potential

Chemical Equation	E^o, Volts
$0.5\ Mn^{IV}O_2\ (s) + 2\ H^+ + e^- \leftrightarrows 0.5\ Mn^{2+}\ (aq) + 2\ H_2O$	$+1.23$ [a]
$Mn^{III}OOH + 3\ H^+ + e^- \leftrightarrows Mn^{2+}(aq) + 2\ H_2O$	$+1.51$ [a]
$2\ Mn^{III} + 2\ H_2O \leftrightarrows Mn^{II} + MnO_2\ (s) + 4\ H^+$	$+0.53$ [b]
$Mn^{III} + e^- \leftrightarrows Mn^{II}$	$+1.51$ [b]

a   Cited from A. Stone (1987) [29]
b   Cited from Kostka et. al (1995) [52]

3. Synthetic Organic Micropollutants

3.1. General Properties and Structure

A complex variety of chemical conditions affect the occurrence and chemical reactivity of organic micro-pollutants in the environment. The work presented in this thesis focused on four organic compounds: phenol, aniline, triclosan, and bisphenol A. Phenol and aniline were chosen as they are model organic compounds and are usually present as the reactive sites on most EDCs. Vast amount of studies have been carried out on these model compounds.[26,28–30,34,53] Triclosan and Bisphenol A are examples of well-known

8

EDCs and their occurrence has been well recorded in natural and engineered water systems; these are biphenyl compounds in which the phenolic moieties are the reactive site. [7,13,55–57]

Phenol is an industrial chemical which is an important raw material for other synthetic organic chemicals. It is a parent compound to a lot of other chemicals called the phenolic class. It is produced naturally from distillation of coal tar. Phenol is also manufactured from benzene sulfonation or cumene oxidation. However major source of Phenol in the environment is through automobile exhaust either by photochemical degradation of benzene or direct emission. Phenols are crystalline solids with a melting point of $43^{\circ}C$ and boiling point of $182^{\circ}C$. Phenol solubility in water is 67 g/l at $16^{\circ}C$, also soluble in non-polar solvents [58–60] and the octanol-water partition coefficient (log K_{ow}) is 1.47. [61,62]
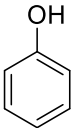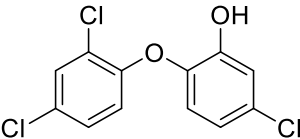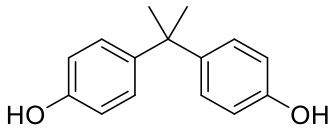
Triclosan (IUPAC name: 5-chloro-2-(2,4-dichlorophenoxy)phenol) is a phenolic chemical that is widely used as an anti-microbial agent and as an active ingredient in many household consumer care products such as soaps, toothpastes, shampoos and cleaning products. Triclosan was brought into use in the 1960's, and first registered as a pesticide with the EPA in 1969. Its use became wide spread after 1972 due to the ban by the Food and Drug Agency (FDA) of the then extensively used antibacterial, hexachlorophene. Triclosan is a crystalline powder with melting point of $54^{\circ}C$ to $57^{\circ}C$. It has a pKa of 7.9, octanol water partition coefficient (log K_{ow}) of 4.76 and poor solubility in water at 10 mg/l. [57,61,62]
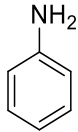
Bisphenol A (IUPAC name: 4,4'-(propane-2,2-diyl)diphenol is another widely used phenolic chemical for the production of plastics like polycarbonates.[55] BPA has also been used for manufacturing flame retardants, paper and paint coatings, adhesives and

9

epoxy resins. It was widely used from the 1930's to the 1990's. In ambient conditions, BPA is a solid crystals with melting point 150°C and solubility of 120-300 mg/l. It has two acid dissociation constants, pKa$_1$ at 9.6 and pKa$_2$ at 10.2. The octanol water partition coefficient (log K$_{ow}$) for BPA measure under ambient pH conditions was 3.40.[56,62–64]

Aniline (IUPAC name: phenylamine) is an important intermediate and raw material for production of various chemicals such as polymers, rubber, pesticides and dyes. They are naturally found in coal tar and manufactured by phenol ammonolysis, chlorobenzene amination or nitrobenzene catalytic reduction. Polyutherane production is one of the major users of aniline. Triclocarban is an antimicrobial produced from aniline which is similar to triclosan and also considered as an emerging contaminant. Aniline is soluble in water (upto 34 g/l) with pKa of 4.63 and the log K$_{ow}$ octanol water coefficient is 0.90.[28,34,61,65] The structure and properties of the micropollutants discussed above are illustrated in **Table 3**.

Table 3. Structure and a few properties of the micropollutants used in this study

Chemical	Structure	Molecular mass (g/mol)	Octanol–water Partition Coefficient (log K$_{ow}$)	Acid dissociation constant (pKa)
Phenol	OH	94.11	1.47	9.89
Triclosan	Cl, OH, O, Cl, Cl	289.54	4.76	7.9
Bisphenol A	HO, OH	228.29	3.40	9.6 [a] 10.2 [b]

10

| Aniline | NH$_2$ structure | 93.13 | 0.90 | 4.63 |

a   pKa$_1$ [56]
b   pKa$_2$ [62,63]

3.2. Occurrence of micropollutants in natural and engineered systems

Organic micropollutants (e.g., Triclosan and BPA) are discharged in the waste water systems due to disposal of pharmaceuticals and personal care products.[3,5,64,66] It was estimated that 109 tons of BPA was reported as releases to air, surface water or wastewater treatment plants in 1993.[56,63] Apart from the releases, the leaching of chemical from products such as bottles containing BPA has been well reported.[55,67] Triclosan and other phenols which are used in personal care products are usually disposed down the drain [66] resulting in contamination of many surface water systems. A national survey of 139 streams demonstrated in the presence of these micropollutants in 80% of the streams, triclosan being one of the most frequently detected (57.6% of streams) with a maximum concentration of 2.3 μg/l, Bisphenol A was detected in 41.2% of the streams (maximum concentration was 12 μg/l). Phenol was observed in 8.2% of the streams and 4-nonylphenol (substituted phenols) was found in 50.6% of the streams with maximum concentration of 40 μg/l.[5].

Micropollutants have also been detected in engineered systems such as drinking water treatment plants and wastewater treatment facilities. The presence of estrogenic micropollutants was surveyed in seven sewage treatment plants receiving primarily domestic effluent.[68,69] Natural hormones 17β-estradiol and estrone were present in all seven plants at concentrations levels of 1 ng/l to 50 - 80 ng/l. Synthetic hormone 17α-

11

ethynylestradiol was present in 3 out of 7 of the sewage treatment plants. Artificial sweeteners, an indicator for micropollutants/wastewater in source water, were present in 13 out of the 17 drinking water treatment plants' finished water stream.[70] Caffeine and artificial sweeteners were also observed in 65% of groundwater samples, indicating wastewater influence on source water.[71,72] Further review[3,73] of micropollutants occurring in wastewater effluents has been conducted in various facilities and the poor removal efficiency has become a concern for the wastewater treatment sector.[2,12]

3.3. Regulations for micropollutants.

The section 304 (a) of Clean Water Act requires establishment of water quality standards, which is prepared by EPA and regularly updated for approximately 150 pollutants. The most recent (2015) Ambient Water Quality Criteria (AWQC) lists phenol in the Human Health Criteria table (significant risk to humans) and the Organoleptic effects table (taste, odor, and color of water). The 2015 EPA human health AWQC standard for consumption of water by humans and organisms is 4 mg/l and the AWQC standard for organism only consumption is 300 mg/l. The 2015 EPA Organoleptic effect criteria is 300 μg/l. Also, the section 112 of 1990 Clean Air Act Amendment, lists phenol and aniline amongst 334 chemicals as hazardous air pollutants. EU has banned phenols in cosmetics since 2006 including manufacturing and distribution. According to European Commission (2007), EU nations should control the emission of phenol to the environment if necessary so that there are no risks to humans exposed via the environment. Denmark has set water quality criteria for phenol at 7.7 μg/l for fresh waters, 0.77 μg/l for marine waters, and 0.5 μg/l for groundwater.

12

In the USA, there has been no federal restriction on Triclosan. However, the state of Minnesota has banned its use in most consumer products (effective 2017). FDA regulates use in personal care products, EPA regulates use as pesticides. EU commission have made severe restrictions on the use of triclosan in personal care products in 2014 with Regulation (EU) No 358/2014, which identifies continued use of triclosan as not safe for consumers, and setting a maximum concentration limit of 0.3% in toothpastes, hand soaps, body washes and deodorants, and a maximum concentration of 0.2% for mouthwashes.

The EPA has added BPA to the Concern List of Toxic Substance Control Act (TSCA) in 2010, where it will be scrutinized for future regulatory action. Bisphenol A in bottles and packaging material is under the jurisdiction of FDA who in 2012, through Docket No. FDA-2012-F-0031 banned the use of BPA containing plastics in infant feeding bottle, sippy cups. Also in 2013, the FDA (Docket No. FDA-2012-F-0728) banned the use of BPA based epoxy resin for packaging of infant formula. Since June 2011, the EU has banned the production and sale of BPA-based polycarbonate baby bottles. However the European Food Safety Authority (EFSA) has confirmed that human health concerns from BPA exposure is not of concern as human exposure to BPA is considerable below the safe intake level. In addition to the EU law, France decided to implement complete ban on BPA in any food packaging from 2015.

The National Water Quality Criteria by US EPA for protection of freshwater aquatic organisms from Aniline is a maximum four day average concentration of 14 µg/l and a maximum one hour average concentration of 28 µg/l. The quality criteria for protection of saltwater organisms for aniline is a maximum four day average of 37 µg/l and

13

a maximum one hour average of 77 μg/l. In Europe, the EU Commission Regulation (EC) No 790/2009 bans to use of various anilines in cosmetic products.

4. Application of $MnO_x(s)$ for water treatment

Conventional processes such as chemical oxidation have been frequently used in water treatment facilities. A chemical oxidant is added to react with inorganic species and hazardous organic chemicals to yield less hazardous oxidized products. Some examples of typical chemical oxidants are Cl, ClO_2, $KMnO_4$ and O_3.[14,74] Common inorganic species in water are Fe(II), Mn(II), and As(III) which can be removed by chemical oxidation.[74,75] Insoluble Fe(III) and Mn(IV) species can also enhance performance of coagulants and filters used downstream to provide separation of the now insoluble species from water. The EPA secondary contaminant levels for Mn are 0.05 mg/l. However, Mn(II) has been found to make its way through the treatment train either due to inefficient removal/oxidation and formation of colloidal species. Studies have identified Mn deposition onto dual filter media (e.g., anthracite and sand), by abiotic sorption and oxidation.[38] Coating of MnO_x is formed on the filter media by a process known as the natural greensand effect.[36,74] This has been found to occur within weeks on new uncoated filter media during normal operation. Merkle et. al[38] observed that this $MnO_x(s)$ coating consisted of birnessite and Al-Mn oxide hydrate from powdered X-ray diffractogram analysis of samples taken from water treatment facility. Limited research has investigated the effect of reactions of organic compounds on the chemical composition and structure of $MnO_x(s)$.[26,32] Thus, more research is necessary to investigate the mechanisms for the interaction of $MnO_x(s)$ with organic micropollutants to further assess the feasibility of this process for water treatment applications.

14

5. Interaction of Organics Micropollutants with $MnO_x(s)$

The reactivity of $MnO_x(s)$ with various organics has been extensively reported in literature.[26,29,76] Some studies indicate that $MnO_x(s)$ acts as a catalyst during the transformation of organics,[30,77] while most studies have identified the dissolution of Mn taking place due to redox reaction resulting in degradation of the organic compound.[19,29,76,78] There are multiple potential chemical pathway suggested such as free radical oxidation, addition of substrate to quinones, complete oxidation to carbon dioxide, sorption onto $MnO_x(s)$ surface and microbial driven redox mechanism.[26,34,44] A summarized reaction mechanism of phenols and aniline with $MnO_x(s)$ is shown in **Figure 1**. The micropollutants, after getting sorbed onto the $MnO_x(s)$ surface, get degraded due to formation of a radical which can either react with other formed radicals to produce polymeric products.[26,31,34] Alternatively, a second electron transfer can take place, resulting in formation of quinones.[26]

The reaction of $MnO_x(s)$ with phenol causes the reductive dissolution of Mn in the solid phase; the dissolution of $MnO_x(s)$ depends on the substituted group on the phenol ring due to electrophilic and steric effects.[29] Another study showed the decrease in reactivity of $MnO_x(s)$ with triclosan when secondary metal oxides such as Al, Ti oxides are present in the $MnO_x(s)$ surface.[79] The transformation of triclosan and chlorophene on reaction with $MnO_x(s)$ is hypothesized that the oxidation occurs at the phenol moiety producing hydroquinone products along with trace amounts of 2,4-dichlorophenol which suggests breaking of the ether bonds.[31,80] Similar studies on the oxidation of BPA and BPF (respectively) by $MnO_x(s)$ with change in pH, humic acid concentration and cations (Ca^{2+}, Mg^{2+}, Mn^{2+}) suggests that metal cations inhibited the reaction with Mn^{2+} being the most

15

suppressive.[67,81] Humic acid had negligible inhibition on BPA reaction with MnO_x(s), but it showed significant inhibition for BPF removal by MnO_x(s) at lower pH (<5.5). Studies identified the major product as hydroquinone along with other intermediates which were formed by radical coupling, substitution, fragmentation and elimination.[67,81,82] Laha and Luthy[28] studied the reaction between MnO_x(s) and various aromatic amines (ie. aniline and substituted anilines), showing the effect of substituted groups on aniline degradation rates and oxidative product formation. Zhang et al. [25] carried out kinetic modelling of MnO_x(s) oxidation of 21 antibacterial compounds categorized into phenolic, aromatic N oxides, flouroquinolonic and tertracyclines. The model parameters were reaction rate and total surface reactive sites which were correlated to effect of reactant and co-solute concentrations and pH. The differences in findings of the mechanistic studies is due to the limitations in detection limits, identification of reaction intermediates and other factors further discussed in the following section.
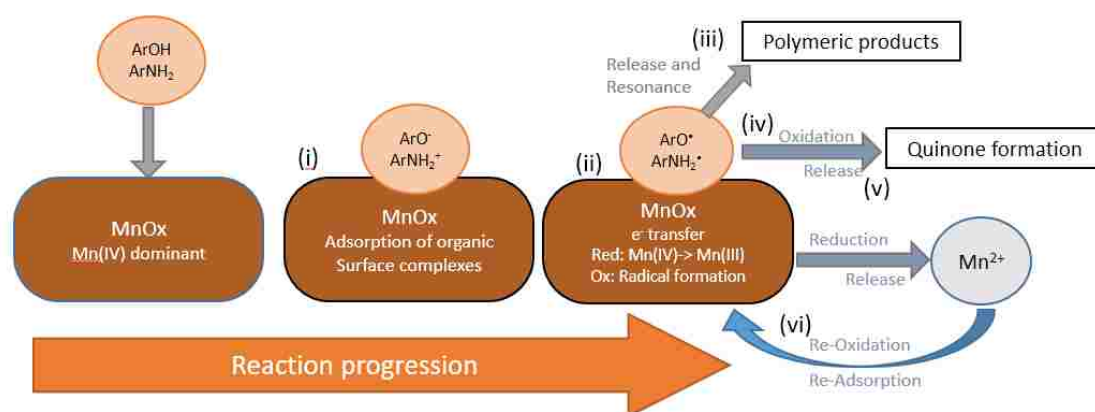
Figure 1 Proposed reaction mechanism for reaction of Phenols (ArOH) and Aniline (ArNH) with MnO_x

6. Research Methods

6.1. Solid Phase Analyses to Investigate Interfacial Organo-Metallic Reactions

Solution phase analyses such as chemical acid digestions analyzed with inductively coupled plasma mass spectrometry (ICP-MS) has been traditionally used to determine total elemental composition. However the changes in Mn oxidation state occurring in the near surface can't be detected with these methods and, therefore, have not been sufficiently studied.[26,83] The advances made in spectroscopic techniques which have enabled researchers to overcome these problems.

The poor crystallinity and similar diffraction pattern of many $MnO_x(s)$ minerals represent major challenges for the identification of different $MnO_x(s)$ phases.[39] However, application of a combination of techniques such as high resolution transmission electron microscopy (TEM), X-ray absorption fine structure (XAFS) spectroscopy, and thermogravimetric analysis (TGA) can facilitate the improved understanding of $MnO_x(s)$ minerology.[42,43] XPS can be a useful tool to detect the oxidation state of Mn in the near-surface of solid samples; narrow scans of XPS Mn 2p, Mn 3p and Mn 3s regions can be used to determine Mn oxidation states.[36,54,83–85] Additionally, XPS analyses can also be used to identify organic functional groups by making narrow scans of the C 1s and O 1s spectra.[78,86,87] Infra-red spectroscopy and Raman spectroscopy can also be useful to identify sorbed molecules on surfaces and oxidation states of metals, and type of carbon-oxygen bonding.

17

6.2. Organic Chemical Analyses

One of the major challenges in research involving micropollutants is the difficulty to analyze them due to their trace concentrations (<1 μg/l).[2] There are few analytical methods which could detect these contaminants in the concentration levels which are environmentally relevant. Also, presence of dissolved solids and other species in the water matrix of environmental samples affects the detection capability of these micropollutants. Advanced spectroscopic and chromatographic techniques have been developed in recent years to help improve the detection limits for these micro-pollutants. New methods for detection of organic micropollutants in aquatic environmental matrixes such as Large volume injection liquid chromatography tandem mass spectrometry (LVI LC-MS/MS) have demonstrated excellent detection limits (1.2 parts per trillion or ng/l) with method accuracy ranging from 88% upwards and low relative standard deviation (12%).[4,88] The variation in properties in each class of these micropollutants suggests that the use of combination of methods/techniques would be most likely to accurately detect and quantify the micropollutants.[2] More volatile compounds have been detected and quantified by gas chromatography with tandem mass spectroscopy (GC-MS/MS), while less volatile and more polar compounds have been detected and quantified with liquid chromatography with tandem mass spectroscopy (LC-MS/MS).[11,70] These recent developments in solid-phase and liquid-phase analysis has enabled the scientific community to examine the gaps in existing body of literature.

18

7. Research Gaps

The knowledge about the changes in chemical composition and structure of $MnO_x(s)$ occurring after reaction with organic compounds is limited in the literature. Current literature focusses on changes happening in the solution, emphasizing on organic reactants. However, the potential effects of organic adsorption on $MnO_x(s)$, the reaction and subsequent release of organic reaction products need to be investigated in more detail. Further research is required to determine the changes in Mn oxidation state and effect of Mn(III) and Mn(II) on performance of $MnO_x(s)$ reacting with organic micropollutants.[26] It should be noted that most studies utilize synthesized media which are pure and not representative of the naturally occurring manganese oxides.[79] Little information is available about the effects of surface area and impurities on $MnO_x(s)$ surface on its reactivity with organic micropollutants. Additionally, organics could compete with organic matter and other metals/anions present in water for $MnO_x(s)$ surface sites.[32] All these factors would affect the long-term reaction rates, while current research focusses on initial kinetics of organic micropollutant removal. There is also a need for identification of reaction products and surface complexes to help in development of kinetic models and accurate reaction mechanism. These limitations and gaps in current research need to be addressed in order to improve our understanding of $MnO_x(s)$ reaction with organic contaminants and establish a scientific basis for application of $MnO_x(s)$ in water treatment and organic micropollutant remediation systems. These knowledge gaps justify the need for the investigation presented in this thesis.

19

<center>Chapter 3</center>

Spectroscopic Investigation of Interfacial Interaction of Manganese Oxide with

Triclosan, Aniline, and Phenol

Nabil Shaikh[1], Saru Taujale[2], Huichun Zhang[2], Kateryna Artyushkova[3], Abdul-Mehdi S. Ali[4], and José M. Cerrato[1]

[1] Department of Civil Engineering, MSC01 1070, University of New Mexico, Albuquerque, New Mexico 87131, USA

[2] Department of Civil and Environmental Engineering, MSC01 1070, University of New Mexico, Albuquerque, New Mexico 87131, USA

[3] Department of Chemical Engineering, MSC01 1120, University of New Mexico, Albuquerque, New Mexico 87131, USA

[4] Department of Earth and Planetary Sciences, MSC03 2040, University of New Mexico, Albuquerque, New Mexico 87131, USA

ABSTRACT: We investigated the reaction of manganese oxide (MnO_x) with phenol, aniline and triclosan using X-ray photoelectron spectroscopy and Raman spectroscopy. The surface of unreacted MnO_x (control) and reacted MnO_x were examined for variations in Mn oxidation state and carbon/oxygen bonding. An increase of Mn(III) and Mn(II) was detected in surface of MnO_x reacted with organics, indicating reduction of MnO_x and presence of stable Mn(III). Reaction of phenol with MnO_x resulted in increase in C-OH bonds (12.5% C 1s), indicating the presence of phenol and its polymeric by-products. Raman spectra confirm this finding with an increased intensity of D and G carbon band compared to control. Detection of chlorine after reaction of MnO_x with triclosan (2.7% Cl 1s increase), suggests that triclosan and its by-products are associated to MnO_x surface. The increase in aromatic and aliphatic carbon bonds after reaction with aniline (20% C1s increase), suggests that aniline and its byproducts are also associated to MnO_x surface. MnO_x reacted with Aniline showed the highest Mn dissolution with 18 μM Mn after reaction completion. The residual parent organic compound in the reactor was highest for

<center>20</center>

Aniline with 3 μM ($k_{aniline}$ = 1 h^{-1}), suggesting that oxidation was the dominant mechanism in Aniline removal. Phenol and Triclosan reacted MnO$_x$ had dissolution of 13 μM and 12 μM Mn respectively. Phenol and Triclosan were completely removed at completion of reaction, with similar removal rates (k_{phenol} = 3.5 h^{-1}, $k_{triclosan}$ = 3.7 h^{-1}), suggesting a combination of sorption and oxidation as mechanism of removal. The results from this research are applicable for the mechanistic understanding of interactions between MnO$_x$ and synthetic organic pollutants.
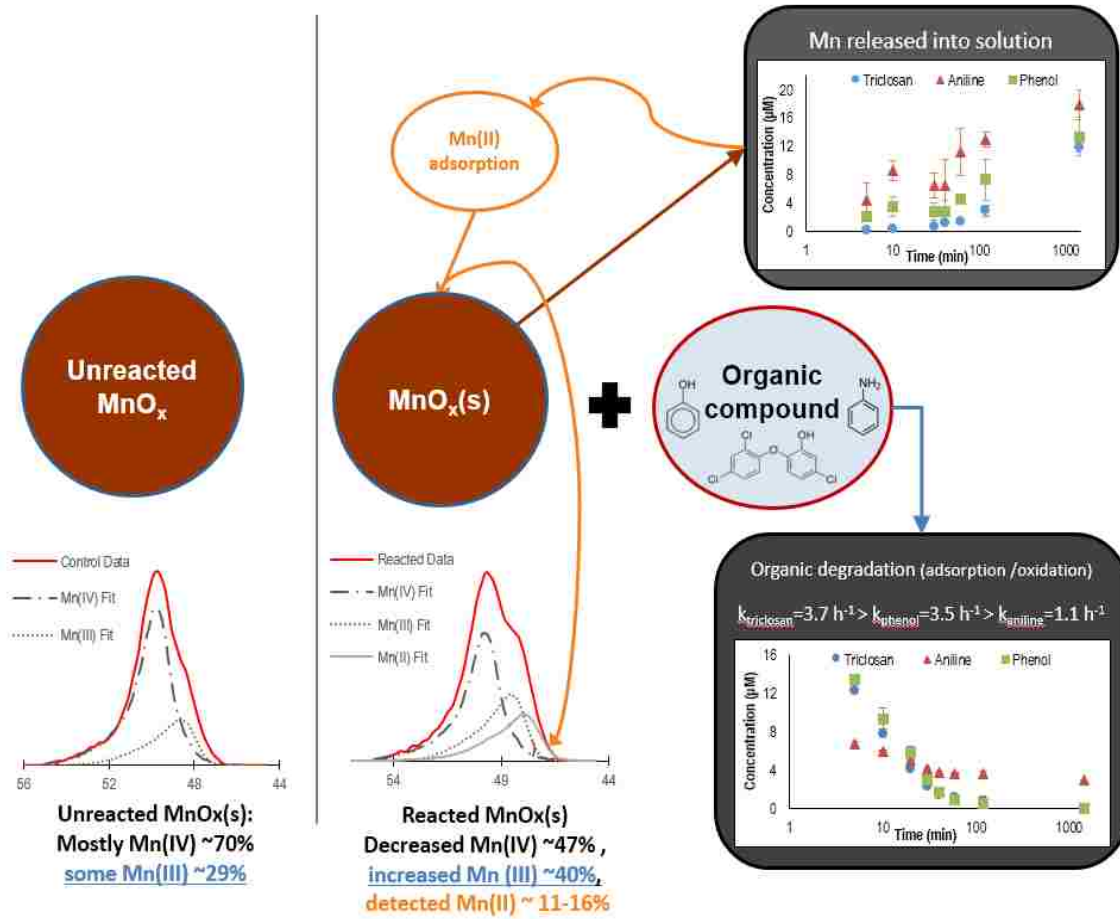
TOC Art.

Figure 2. TOC art: Summarized reaction between the synthetic organics and δ-MnO$_2$

1. Introduction:

Emerging organic contaminants have been increasingly identified in the last few decades in natural waters, waste water, and reused water as a result of daily inputs from anthropogenic activities. Water reuse has become a necessary practice in semi-arid regions experiencing extended dry seasons due to the effects of climate change and increasing population. While reuse practices contribute to the sustainable use of water, a new generation of emerging organic micropollutants (e.g. hormones, pharmaceuticals, and endocrine disrupting compounds) has been increasingly scrutinized.[1,5] Despite the trace concentrations of organic micropollutants,[7,68] new advances in analytical techniques have enabled the detection and quantification of these chemicals in the environment.[89,90] Recent studies show the ill-effects of the increasing concentration of these micropollutants on the ecosphere, especially on aquatic life.[6,8] Olfactory disruption leading to loss of homing behavior, mutation of reproductory organs and retarded growth are examples of negative impacts caused by these organic micropollutants.[8,9,69,91,92] Phenol and aniline are widely used in chemical manufacturing and often found in the environment as pesticides and chemical residues. Due to their toxicity, they have been listed as high priority pollutants by the US EPA.[58] Triclosan [5-chloro-2-(2,4-dichlorophenoxy)phenol] is another chemical widely used as an anti-microbial[57,93] which can cause the development of bacterial resistance[94] and can inhibit lipid synthesis.[95] Additionally, triclosan can degrade due to heat and light forming chloro-dioxins which are highly toxic.[96] Despite the existing evidence on the negative effects of these emerging contaminants, only 25% of waste water treatment plants in the U.S. manage to exceed 1 log removal of these micropollutants.[3]

23

The reaction mechanism of phenolic compounds (ArOH) or aniline (ArNH$_2$) with manganese oxides has been studied as a surface sensitive, two electron overall transfer redox reaction. It can be generalized as follows: (i) adsorption of ArOH/ArNH$_2$ to the MnO$_x$(s) surface [28,29,31,97];(ii) formation of radical ArO•/ArNH$_2$• and reduction of Mn(IV) to Mn(III) on the surface of MnO$_x$[28–30,60]; (iii) release of a fraction of radicals followed by their resonance and formation of polymeric product [26,28,29]; (iv) oxidation of adsorbed radicals to oxidized products and reduction of Mn (III) to Mn(II) [26,28,29,31,98]; (v) release of the redox reaction products from the surface [26,30]; and (vi) adsorption and re-oxidation of Mn(II) on the surface of MnO$_x$[26,53]. Studies show that the reaction of phenols with MnO$_x$(s) produces phneoxy radical which resonates and polymerizes to give polymeric products like phenol dimers, para-substituted benzoquinones and hydroquinones.[26,29] Major product of Triclosan oxidation is 2,4-dichlorophenol along with some p-quinones.[31] Aniline reacts MnO$_x$(s) to produce hydrazobenzene due to head to head coupling of aniline radical which oxidizes further to form azobenzene as the primary reaction product.[28]

Although the oxidation of organic compounds by reaction with manganese oxide [MnO$_x$] has been widely studied[26,60,67,81,99], little is known about the changes in chemical characteristics of the reacted MnO$_x$(s) surfaces.[26] The high reactivity and oxidation strength of manganese oxides make them significant contributors in environmental redox reactions. Several studies have shown the importance of MnO$_x$(s) in abiotic degradation pathway for various phenols [29] and aromatic amines.[28,31] Mn (IV) oxides are often considered as predominant solid species in nature. Mn (III) plays an important role in the redox reaction with organic and inorganic constituents.[35,49,53] Kinetic studies explaining the reaction of MnO$_x$(s) with organic compounds suggest that Mn (III) plays an important role

24

as Mn(III) is more reactive than Mn(IV) due to its faster rate of ligand exchange[53] and higher redox potential.[19,29] Also, Mn(III) is the rate limiting step in oxidation of Mn(II) to Mn(IV).[35,51] However, experimental studies investigating the role of Mn(III) reactivity in redox reactions are limited.[35,50,51,100]Additionally, the changes occurring on $MnO_x(s)$ surface after reacting with organic compounds are not yet completely understood.[26,31]

The objective of this study is to determine Mn oxidation states and the chemical composition of $MnO_x(s)$ after reaction with synthetic organic compounds using XPS and Raman spectroscopy. We have integrated experimental data such as Mn dissolution and organic removal kinetics along with spectroscopic data to investigate the reaction of $MnO_x(s)$ with aniline, triclosan, and phenol and identify changes in the surface Mn oxidation state and chemical composition of reacted and un-reacted $MnO_x(s)$. This study contributes to better understand the reactivity of $MnO_x(s)$ with synthetic organic compounds, which is essential to understand naturally occurring biogeochemical processes and for the development of water treatment technologies that use $MnO_x(s)$ to remove emerging organic micropollutants.

2. Materials and Methods:

Materials. Phenol, aniline and Triclosan (>99% purity) were purchased from Sigma Aldrich (St. Louis, MO). All other chemicals where bought from VWR or Thermo Fisher with >90% purity and used without further purification. Delta manganese dioxide (δ-MnO_x) was used in this study, as it is considered analogous to birnessite.[42,51] Birnessite is the naturally abundant form of manganese oxide[42] arranged as edge sharing MnO_6

25

octahedra with mixed valent manganese centers[53].The δ-MnO$_x$ was synthesized as done by Taujale and Zhang [79] reacting KMnO$_4$ and MnCl$_2$ in basic conditions.

Experiment Set-up. The experiments were performed in 200 ml amber glass bottles. Four different reactors with 10 mM MnO$_x$(s) were prepared and labelled as MnO$_x$-Control, MnO$_x$-Aniline, MnO$_x$-Phenol and MnO$_x$-Triclosan. 0.01 M NaCl was added to each to provide counter-ions and the pH was constantly monitored and adjusted to 5.0 using hydrochloric acid and sodium hydroxide. 1.0 mM of aniline, phenol, and triclosan were added to each respective reactor and the reactor without addition of organic compound was the control. The batch reaction conditions are illustrated in **Figure S1**. The reactors were then stirred for four hours and left over night to settle. After decanting and discarding the supernatant, the remaining suspensions were centrifuged at 12,000 g for 20 minutes. The supernatant was discarded and the settled particles were collected for solid analysis. Samples of 1 mL and 10 mL aliquots were collected at different time points (5, 10, 20, 30, 40, 60, 120 and 1440 minutes, respectively) for all reactors. 25 μL 1M NaOH was added to all 1-mL aliquots to quench the reaction and desorb all unreacted organics so that the measured loss of the organics was only due to oxidation,[31] after filtration through 0.22 μm membranes, the samples were analyzed by HPLC coupled with a DAD detector for the concentrations of aniline, phenol, and triclosan. The 10 mL samples were filtered through 0.22 μm membranes, acidified with HNO$_3$, and analyzed by ICP-MS for Mn^{2+} ions.

Kinetics: The oxidation kinetics of the organics were fitted into pseudo-first order kinetics for removal of organic contaminants in reactor. d[c$_{org}$]/dt = k × [c$_{org}$] where c$_{org}$ is the

26

concentration of the organic reactant in the reactor and k is the pseudo-first order rate constant.

X-ray Photoelectron Spectroscopy (XPS). XPS was used to identify surface composition and oxidation state of elements in the near surface. XPS spectra were acquired on a Kratos Axis DLD Ultra X-ray photoelectron spectrometer using a monochromatic Al Kα source operating at 225W with no charge compensation. Spectra were obtained from three different areas on each sample. Elemental survey spectra were acquired at 80 eV and high resolution at 20 eV pass energy. Data analysis, curve fitting and quantification were performed using CasaXPS software. Narrow scan XPS spectra were processed using Shirley background subtraction and a Gaussian-Lorentzian line shape for the curve-fit of spectra.[83,84] Calibration was carried out using gold powder deposited on each sample with respect to the position of the Au $4f_{7/2}$ peak (at 84.0 eV). Pure (>99%) manganese oxides (MnO, Mn_2O_3, MnO_2 and Mn (III,IV) oxide) were purchased from Strem Chemicals (Newburyport, MA) and Sigma Aldrich (St. Louis, MO). Oxidation states of Mn were determined using the Mn 3s multiplet splitting method and by examination of the shape and position of the Mn 3p region as described by Cerrato et al.[36,83] Analyses of C 1s and O 1s peaks were done based on results obtained from other studies.[86,87,101] The limits of detection for survey scans were 0.1% and the precision of XPS was ±0.1 eV.

Raman Spectroscopy. All Raman spectra were acquired on a WITec Alpha 300R confocal Raman microscope with 532 nm laser excitation. Samples were prepared as powders on a glass slides, with the excitation laser focused through at 10x and 50x microscope objective for a total spot size of ~0.1 micron. Excitation power was held constant at ~150 μW for all samples. A grating of 600/mm was used with spectral resolution of 0.5 cm^{-1}. Each

27

spectra has 50 accumulations with integration time of 0.63894 seconds. Spectra were fit using Project Four software. The spot size was calculated as: NA× $\lambda/2$; where NA is numerical aperture and λ is laser wavelength. 10x and 50x has a NA of 0.24 and 0.75 respectively. So the sampling depths were 63.84 nm and 199.5 nm.

3. Results and Discussion

Surface Elemental Composition. The near surface (top 5-10 nm) elemental composition was quantified using XPS survey scan mode (**Table 4**). The carbon (C) content for the unreacted sample (MnO_x-Control) was 26.2%, likely due to the contribution of adventitious carbon. For the reacted samples, there is an increase in the percentage C for MnO_x-Aniline (40.9%), MnO_x-Phenol (39.4%) and MnO_x-Triclosan (39.6%), suggesting the possible association of the organic compounds to the $MnO_x(s)$ surface. Because the parent compounds have been mostly oxidized when the oxide samples were collected, the surface associated organics are mostly oxidation products. Similar Mn contents were measured for MnO_x-Aniline (18.7%), MnO_x-Phenol (19.9%), and MnO_x-Triclosan (19.5%), which are within 1.3%. In contrast, the Mn content for the unreacted MnO_x-Control sample was 25.4%. Consistent with the increase in C observed for all the MnO_x reacted sample, the decrease in its Mn composition suggests that the surface sites of MnO_x media are occupied by the parent organics and their oxidation products. Chlorine is detected only on the surface of MnO_x-Triclosan, at 2.7%, suggesting that triclosan reaction products are associated to the surface of MnO_x. Despite the similar C and Mn content on the surface of the reacted samples (within 1.5% of each other), the rate of removal of organics and Mn release were observed to be different. This contrast could be due to differences in reaction kinetics, or

28

due to different reaction mechanisms as discussed more extensively in the following sections. For aniline reacted samples, a slight increase in nitrogen content also indicates the presence of aniline and its products on the surface of the media.

Manganese (Mn) XPS narrow scans. XPS analyses suggest that Mn reduction in MnO_x occurred given that an increase of Mn(III) was detected in all reacted MnO_x samples compared to the initial content detected on the unreacted MnO_x (control). The XPS Mn 3s multiplet splitting was obtained for unreacted and reacted MnO_x samples, and for Mn(II), Mn(III), and Mn(IV) reference materials (**Table 5**). The unreacted control sample had a multiplet splitting of 4.6 eV, which is within 0.22 eV of the multiplet splitting of 4.4 eV obtained for the Mn(IV) reference. The multiplet splitting of the aniline samples (4.9 eV) coincides with the Mn(III, IV) reference. Additionally, the same multiplet splitting of 4.8 eV was obtained for the phenol and triclosan reacted samples, which is within 0.1 eV of the Mn(III, IV) reference. From the Mn 3s multiplet splitting data in this study, the Mn in unreacted MnO_x has an average oxidation state of 3.7. This value is consistent with other studies[29,53,102]. For example, the average oxidation state of the Mn in birnessite is 3.6 to 3.8 due to the presence of Mn(III) among the dominant Mn(IV) species.[29,102] Hence, the unreacted MnO_x is not pure Mn dioxide, with the molecular formula being around $MnO_{1.8}$ to $MnO_{1.94}$.[53] The average Mn oxidation states for the MnO_x reacted with aniline, phenol and triclosan are 3.2, 3.4 and 3.3, respectively.

The Mn 3p photopeak for the reacted samples match well with the Mn(III, IV) reference (**Figure 3 b-d**), suggesting that Mn reduction occurred during the reaction of MnO_x with the organic compounds, and the Mn(III) concentrations in the surface increased as compared to the unreacted sample. The shift of the Mn 3p spectra to lower binding

29

energy (BE) suggest presence of Mn(II) in the surface. The photoline for MnO_x-Control closely matches up with the Mn(IV) reference, with some of the Mn(III) features at around 48.5 eV (**Figure 3a**). The percent contribution of Mn(IV), Mn(III), and Mn(II) in the Mn 3p spectra of unreacted and reacted samples (**Figure 3e**) was determined based on curve-fitting and quantification of the Mn 3p narrow scans (shown in **Figure S2**). This is obtained by fitting the Mn 3p spectra of the samples with Mn 3p spectra for Mn(II), Mn (III) and Mn (IV) pure references. A significant increase in % Mn(II) can be seen from fitting the 3p spectra of reacted samples, with MnO_x-Aniline (16.6%), MnO_x-Phenol (11.9%), MnO_x-Triclosan (12.8%) compared to the undetectable amount in MnO_x-Control. The average oxidation state from the curve-fitting was calculated for MnO_x-Control (3.7), MnO_x-Aniline (3.3), MnO_x-Phenol (3.4) and MnO_x-Triclosan (3.3). The data from Mn 3p for average surface oxidation state of MnO_x-Control and reacted species is consistent with the Mn 3s multiplet data. Thus these results suggest that Mn reduction takes place, with reduced species (Mn(III), Mn(II)) present as adsorbed species after reaction completion. The presence of stable Mn(III) is a notable observation here. Additional C 1s and O 1s high resolution spectra were analyzed below to better understand the C and O bonding at the surface of MnO_x(s) reacted and unreacted samples.

Carbon (C) and Oxygen (O) XPS narrow scans. Fitting of the C1s and O1s high resolution spectra was performed to analyze the different types of C and O species present in the near surface of the reacted and unreacted samples, which are shown in **Figure 4**. The percent composition of each C and O species obtained from the fits of the C 1s and O 1s high resolution spectra are given in **Table S1** and **Table S2** respectively. The binding energy positions for the corresponding C and O species observed in this study are consistent with

30

those reported in other studies.[86,87,101] All the samples were within 1.5% from each other for the C=O carbon bonds indicating a lack of ketones/aldehydes on the surface.

The unreacted (MnO_x-Control) sample had the highest percentage of secondary carbon (C^*-CO_x/C^*-CN_x) on the surface. All the reacted samples showed increase in aliphatic/aromatic carbon (C-C/C=C), indicating towards increased organic presence on the surface of MnO_x(s) with MnO_x-Phenol having the highest (70%) followed by MnO_x-Aniline (65.4%) and MnO_x-Triclosan (62.1%). Analyses of the C 1s high resolution XPS spectra suggest that both MnO_x-Phenol and MnO_x-Triclosan have similar features, suggesting similar binding characteristics (all fits for different carbon bonds were within 10% of each other). An increase of 16% was detected on the C-C/C=C bonds and a decrease of 13% for the C^*-CO_x bonds was detected for MnO_x-Aniline as compared to the unreacted MnO_x-Control.

The MnO_x-Triclosan and MnO_x-Phenol sample had higher percentage of C-OH bonds detected in the near surface region compared to other samples, particularly an increase of 8% and 6% respectively compared to control sample, suggesting that phenolic reaction products are present on the surface of MnO_x with association at the para position of the phenol ring ($>MnO_x$-C_5H_5-C-OH). However, MnO_x-Phenol reacted samples show a 25% decrease in C^*-CO bonds while MnO_x-Triclosan show a 15% decrease in C^*-CO bonds when compared to the MnO_x-Control (11.1% and 8.3% respectively). Additional XPS analyses were performed on the O 1s high resolution spectra to better understand oxygen bonding characteristics.

The XPS O 1s high resolution spectra for MnO_x-Control showed surface composition of metal oxide (MnO_x) at 55.5%. In contrast, we observed a decrease in MnO_x

31

bonds on the surface of all the reacted samples with the lowest being MnO_x-Phenol at 44%, followed by MnO_x-Triclosan at 48.6% and MnO_x-Aniline at 50.6%. This agrees with the decrease in Mn composition on reacted MnO_x surface observed in the survey scans. The shape of O 1s spectra is similar for the MnO_x-Aniline and MnO_x-Triclosan. Fitting of these high resolution O 1s spectra suggest that there was a comparable amount of oxygen double bonded to N or C (O=N-C / O=C), in MnO_x-Aniline (29.7%) and MnO_x-Triclosan (28.4%), with respect to 30.2 % in the unreacted control. There was an increase in C-OH bonds for MnO_x-Triclosan (14.0%) compared to MnO_x-Control (10.3%), which is consistent with the increase of C-OH bonds seen in C 1s high resolution spectra analysis. These results for MnO_x-Triclosan are consistent with those reported in previous studies which observed the formation of dioxins, quinones and triclosan dimers after oxidation reaction of triclosan.[31,93,96]

The shape of the O 1s XPS spectra for MnO_x-Phenol is unique compared to all other samples (**Figure 4)** given that it has noticeable shoulders at a binding energy range from 530.6 eV to 535.4 eV. These shoulders result from the contributions of the C-O-O-C bonds (peak 535 eV) on the surface, which is absent from all other samples. Additionally, MnO_x-Phenol had the highest composition of C-O-C/COOH bonds (13.4%, compared to 4% in control, 8.4 % in aniline, and 8.0% in triclosan) and C-OH bonds (15.9% compared to 10.3% in control, 11.3% in aniline, and 15.0% in triclosan). This finding in the XPS O 1s high resolution spectra is consistent with the observed increase of C-OH bonds observed in C 1s high resolution scans. These results confirm the presence of products of phenol polymerization associated to the surface after the reaction of phenol with MnO_x reported

32

in other studies.[29,98] Additional Raman spectroscopy analyses were conducted to further analyze the surface of unreacted and MnO_x-Phenol reacted samples.

Raman Spectroscopy. Single scan data from various locations on MnO_x media for the unreacted control and phenol reacted samples are illustrated in **Figure 5**. The presence of manganese oxide is noticeable with the peak at $610 \ cm^{-1}$. The MnO_x-Control sample spectra has peaks at $2900 \ cm^{-1}$ corresponding to C-H bonds and the peaks at $1350 \ cm^{-1}$ and $1600 \ cm^{-1}$ due to diamond and graphite (D and G) bands which could be adventitious carbon or the acetic acid buffer used for the experiments. Most MnO_x-Control single spectra do not show these carbon bands, apart from in a few single scans which can be attributed to the acetate buffer used. However, in the MnO_x-Phenol sample, the D and G carbon bands are present in all the Raman spectra, suggesting that organic groups are present in the MnO_x surface. This observation is consistent with the XPS data discussed in the previous subsection. It is important to note that Raman spectroscopy scans cover a depth of up to 200 nm, suggesting the possible incorporation of phenol or its oxidation products[77] into the surface of reacted MnO_x. It is possible that the continuous oxidation of phenol in the reacted MnO_x surface results in the reduction of Mn to form both Mn(III) associated with the solid surface and soluble Mn(II) which could re-adsorb to the surface or be released into solution. Surface layers could result from the interaction of reduced Mn and adsorbed organics as the coupling of phenol on the surface results in larger and increasingly hydrophobic polymers[77]. Further measurements of Mn(II) dissolution and removal of organic compounds from the reaction experiments were performed and discussed below.

33

Solution Chemistry Analyses. The removal of organic compounds by MnO_x media was analyzed **(Figure 6b)** and fit according to first order kinetic modelling **(Figure 6c)**. After the initial rapid removal of organic compound (upto 99.9% removal in first 5 minutes) which occurs due to rapid sorption onto un-hindered surface sites and subsequent faster oxidation[25], the removal of organics slows down and shows a good fit to first order kinetics with R squared values greater than 0.98. This slowdown is due to lack of reaction sites and MnO_x surface passivation due to Mn reduction discussed further in the next paragraph. Aniline shows the fastest initial removal as the amount of aniline, phenol, and triclosan remaining at 5 min was 6.74, 13.41, and 12.30 μmol/L, respectively. After 5 mins, the aniline reaction rate slows down compared to phenol and triclosan, with $k_{aniline} = 1.1$ h^{-1}. Both Phenol and Triclosan reacted sample show similar organic removal characteristics with rate constant (5 minutes onwards) of $k_{phenol} = 3.5$ h^{-1} and $k_{triclosan} = 3.7$ h^{-1}. Thus, aniline was still remaining in the reactor (3 μM) while phenol and triclosan were not detected in the samples after 24 hours. This can be attributed to the inhibition of redox reaction between MnO_x media and aniline due to increased presence of Mn(II) on MnO_x surface, which is discussed in the following paragraph.[53]

The Mn released into the aqueous solution for aliquots taken at timed intervals for the different batch reactors were measured using ICP-MS and are illustrated in **Figure 6a**. Given that these experiments were conducted under ambient conditions with limited complexing agents, we assume that the Mn released into solution is mostly Mn(II) as suggested in other studies.[20,50] Compared to the rapid disappearance of the organic from the solution, the data shows that the rate of Mn release is much slower in the first 120 minutes for MnO_x(s) reaction with aniline, triclosan, and phenol (**Figure 6b**). MnO_x-

34

Aniline has the highest Mn release which initially fluctuates up to 50 minutes, after which released Mn increases logarithmically towards a steady state value of 23 μmol/l after 24 hours. This fluctuation can be attributed to two reasons; First, there is rapid reversible adsorption of reacted aniline and reduced Mn onto $MnO_x(s)$ and transformation of Mn(II) to $Mn^{2+}(aq)$ resulting in release of Mn into solution as suggested in other studies.[28,65] As these reversibly adsorbed compounds are released, the aqueous Mn along with other organic compounds are able to re-adsorb on the freshly available surface sites. This process continues until all the surface sites are saturated (irreversibly occupied).[26,28] This finding of the highest Mn dissolution is consistent with Mn surface oxidation state being the lowest for MnO_x-Aniline and the decrease in Mn % in the survey scans. Secondly, this is due to the faster initial oxidation rate of aniline than that of phenol or triclosan, resulting in a greater amount of Mn^{2+} formed initially. Note the starting concentrations of aniline, phenol, and triclosan are between 990 and 1000 μmol/L. Assuming 1-electron transfer between MnO_x and the organics, it means by 5 min, greater than 99.9% of organics have been oxidized, yet only a small fraction of Mn^{2+} have been released to the solution, while majority of Mn^{2+} are still surface associated, as seen by the increase Mn(II) in Mn XPS narrow scans. Furthermore, the slowing of aniline removal and observation of aniline in reactor after reaction completion can be attributed to inhibition due to the higher Mn(II) concentration in solution (as seen above) and on surface seen from Mn 3p fittings.

MnO_x-phenol had the next highest Mn^{2+} release with a logarithmical increase from 2 μmol/l Mn^{2+} after 5 mins to 18.3 μmol/L Mn^{2+} after 24 hours. However, limited fluctuations on Mn released into solution were observed for MnO_x-phenol experiments,

35

unlike the aniline reacted experiments. This can be attributed to the strong adsorption of reduced aqueous Mn to MnO_x.[29,31] MnO_x-Triclosan reacted samples had the least Mn release with a linear increase from 0.1 μmol/l Mn after 5 mins to 15 μmol/l Mn released into solution after 24 hours. Previous work has shown that phenol is more reactive than triclosan towards oxidative transformation by MnO_2, [31] so the reactivity of the organics is not the reason for the observed difference in the soluble Mn released. Despite being phenolic, the low Mn dissolution of triclosan could be due to the electronic withdrawing effect of meta-substituted chlorine and steric hindrance of the large substituent at the ortho position (2,4-dichlorophenolate).[29,31,98] Although the pKa of triclosan (pKa=7.9) is lower than phenol (pKa=9.9), triclosan (log k_{ow}=4.76) is more hydrophobic than phenol (log k_{ow}=1.47) which could result in stronger surface binding.[31] Additionally, triclosan and its oxidation products are greater in size than phenol (and its byproducts) resulting in more surface sites being blocked by triclosan and its oxidation products. While the XPS Mn 3s and Mn 3p analyses suggest that MnO_x-Phenol and MnO_x-Triclosan have the same oxidation state, XPS survey scans show a significant increase in C% and decrease in Mn% for MnO_x-Phenol compared to MnO_x-Triclosan. This indicates greater availability of reactive surface sites in MnO_x-Phenol compared to MnO_x-Triclosan which causes the higher association of carbon groups and dissolution of Mn in MnO_x-Phenol. Thus, these observations suggest that the amount of available surface binding sites is the rate limiting step for oxidation of organic compounds and, subsequently, for re-sorption/re-oxidation of aqueous Mn onto MnO_x as suggested in other studies.[29,98]

36

4. Environmental Implications.

The results of this study emphasize the importance of solid surface analyses in further understanding the different oxidation states of Mn and the bonding of organic groups that take place during the reaction of MnO_x with organic micropollutants. Different changes in the oxidation state of Mn in the MnO_x surface were observed for the reaction with aniline, triclosan, and phenol, indicative of differing mechanism or pathways of surface reactions for different organic groups. Although previous studies had stated that Mn(III) is unstable and only present as a transition oxidation state, the results obtained suggest that Mn(III) was stable in the experiments performed and that it was possible to detect its increase in the surface of MnO_x solids after reaction with organic compounds with XPS analyses.[20,50,103] Another possibility is that Mn(III) in the surface is present in the Mn-bearing solid phases as observed in other studies[50,51,53] Additional research is needed to identify these specific Mn(III)-bearing solid/soluble phases.

The reduction of MnO_x solids [resulting in the increase of Mn(III) and Mn(II) on the reacted surface of MnO_x media coupled with the release of Mn^{2+} into solution] after the reaction with different organic compounds indicates that these solids act as oxidizing agents, not merely catalysts (that is, MnO_x is consumed) during these oxidation reactions. The laboratory experiments and surface analyses presented in this study have important implications towards better understanding biogeochemistry of Mn in both natural and engineering system, and water treatment processes that apply MnO_x solids to remove organic micropollutants. For instance, it is necessary to further understand the role of Mn(III) in the reactivity and oxidation abilities of MnO_x. Additionally, the presence of adsorbed organics and the possible incorporation of these organics into the structure of

37

MnO_x solids, as suggested by XPS and Raman spectroscopy analyses, could play an important role in the reactivity and transport of these organic micropollutants.

5. Acknowledgements

Table 4. XPS survey scans for MnO_x control and reacted samples.

	C 1s %	O 1s %	Mn 2p %	N 1s %	Cl 2p %
MnO_x-Control	26.2 ± 6	47.9 ± 2	25.4 ± 6	BDL	BDL
MnO_x-Aniline	40.9 ± 3	38.6 ± 1	18.7 ± 3	1.4 ± 1.3	BDL
MnO_x-Phenol	39.4 ± 6	40.0 ± 3	19.9 ± 4	0.1 ± 0.6	BDL
MnO_x-Triclosan	39.6 ± 5	37.1 ± 2	19.5 ± 5	0.1 ± 0.6	2.7 ± 0.2

[a] BDL = Below Detection Limit ($<0.1\%$)

Table 5. Results for XPS Mn 3s multiplet splitting for: **a)** Reference Mn oxides; and **b)** control and reacted samples. Curve 1 and curve 2 corresponds to the position/binding energy of ^5S and ^7S for each sample.

	Sample	Curve 1: Mn ^5S (eV)	Curve 2: Mn ^7S (eV)	Multiplet Splitting (eV)
a) References	MnO; Mn(II)	89.10	83.40	5.69
	Mn_2O_3; Mn(III)	88.52	83.20	5.33
	Li Mn(III,IV)O	88.94	84.05	4.90
	MnO_2; Mn(IV)	88.89	84.52	4.38
b) Samples	MnO_x-Control	88.99	84.36	4.63
	MnO_x-Aniline	88.94	84.00	4.94
	MnO_x-Phenol	88.77	83.99	4.78
	MnO_x-Triclosan	88.93	84.12	4.81

40
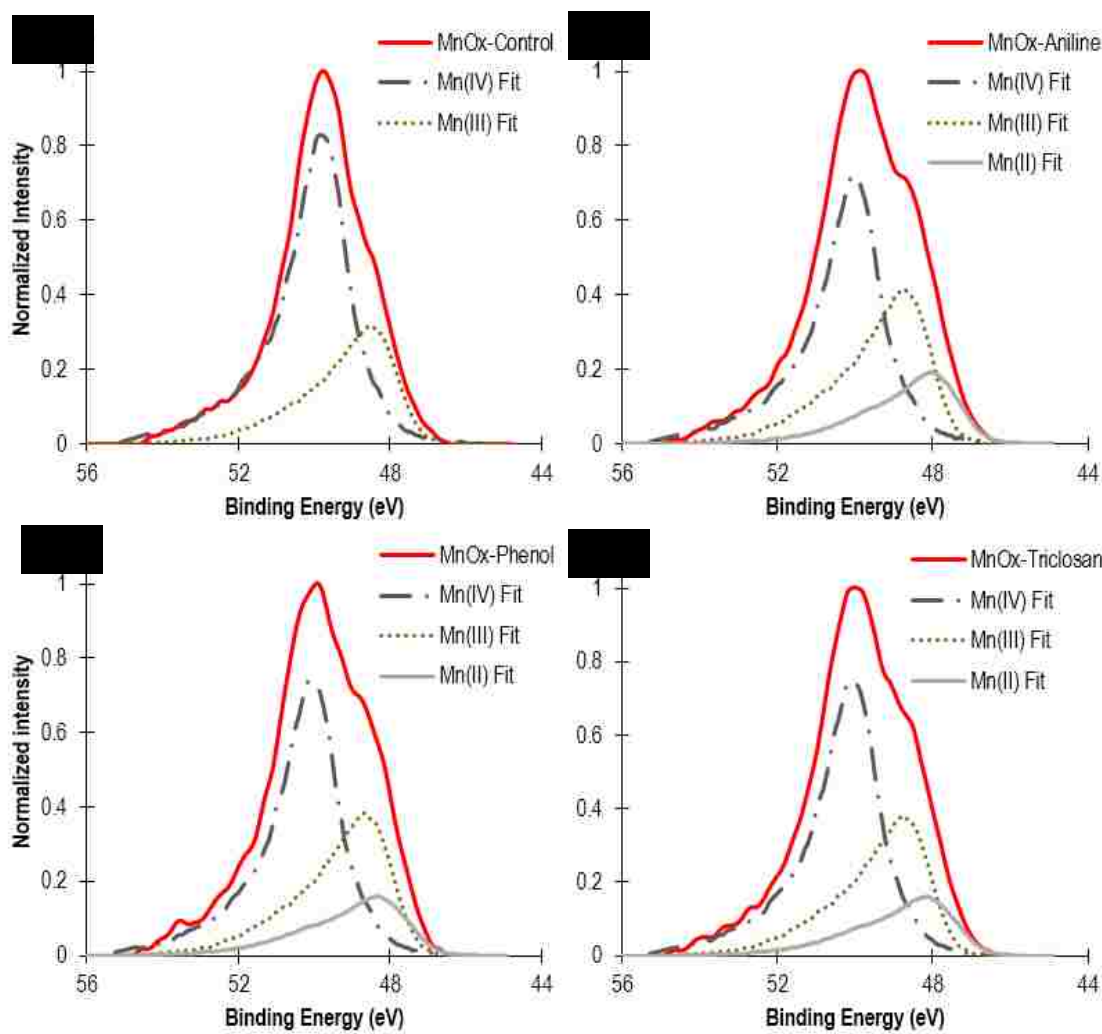
Sample	%Mn(IV)	%Mn(III)	%Mn(II)
MnO$_x$-Control	70.6	29.4	BDL
MnO$_x$-Aniline	46.9	37.9	15.2
MnO$_x$-Phenol	49.6	38.6	11.8
MnO$_x$-Triclosan	46.0	39.4	14.7

[a] BDL = Below Detection Limit

Figure 3. Mn 3p photo-peak for: **a)** MnO$_x$-Control (unreacted); **b)** MnO$_x$-Aniline; **c)** MnO$_x$-Phenol; **d)** MnO$_x$-Triclosan; and **e)** Percent composition of Mn 3p spectra by fitting Mn(II), Mn(III) and Mn(IV) reference spectra. Note that the spectra for unknown samples are shown in red, and for the Mn(II), Mn(III), and Mn(IV) references are shown in grayscale

41
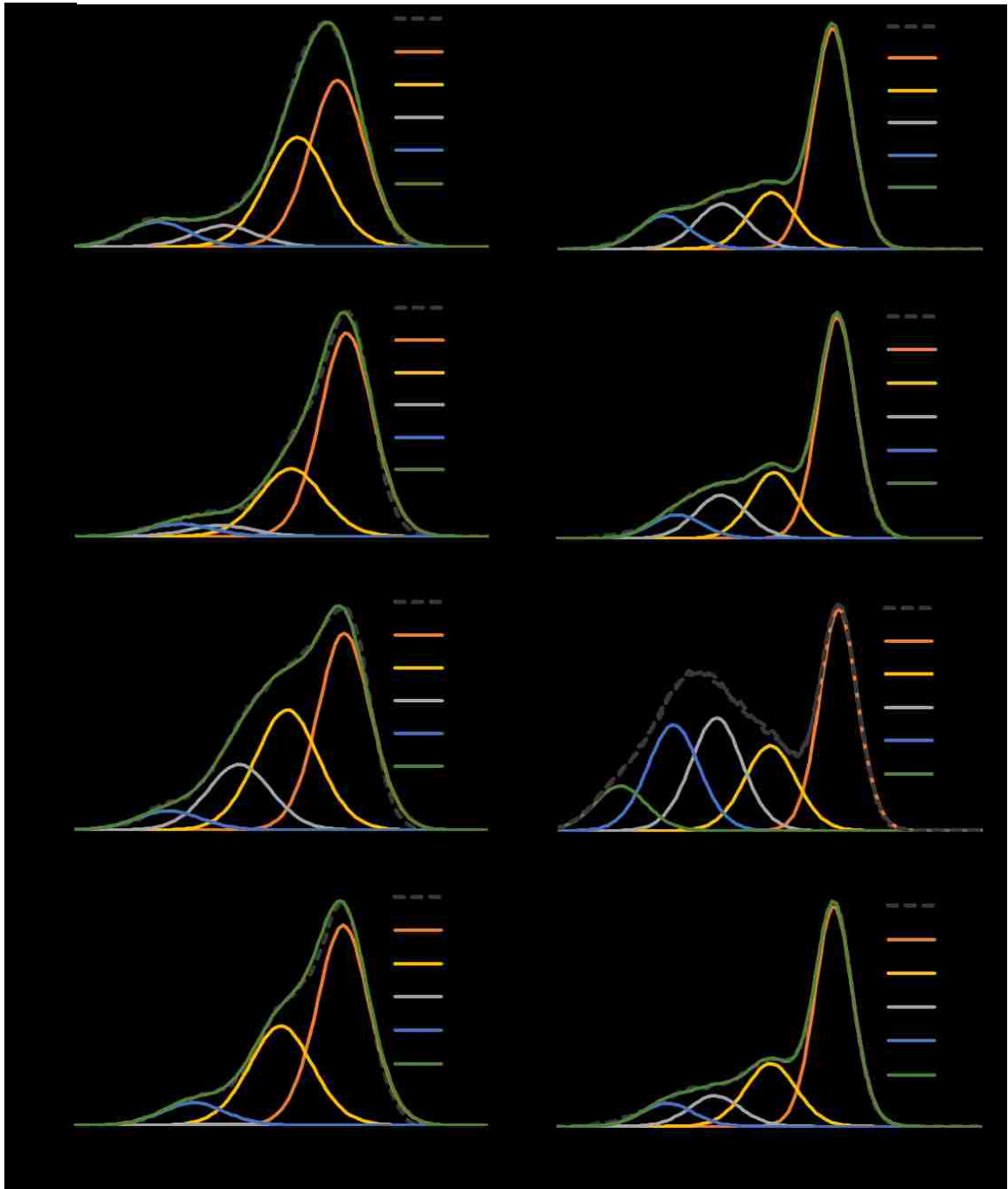
Figure 4. Fitting of XPS C 1s and O 1s spectra with corresponding types of carbon and oxygen bonds based on their signature binding energy for: **a)** MnO$_x$-Control; **b)** MnO$_x$-Aniline; **c)** MnO$_x$-Phenol; and **d)** MnO$_x$-Triclosan. The black dotted line corresponds to XPS data for unknown samples, solid lines correspond to the different types of carbon or oxygen bonds and solid green lines correspond to the composite curve of these bonds.
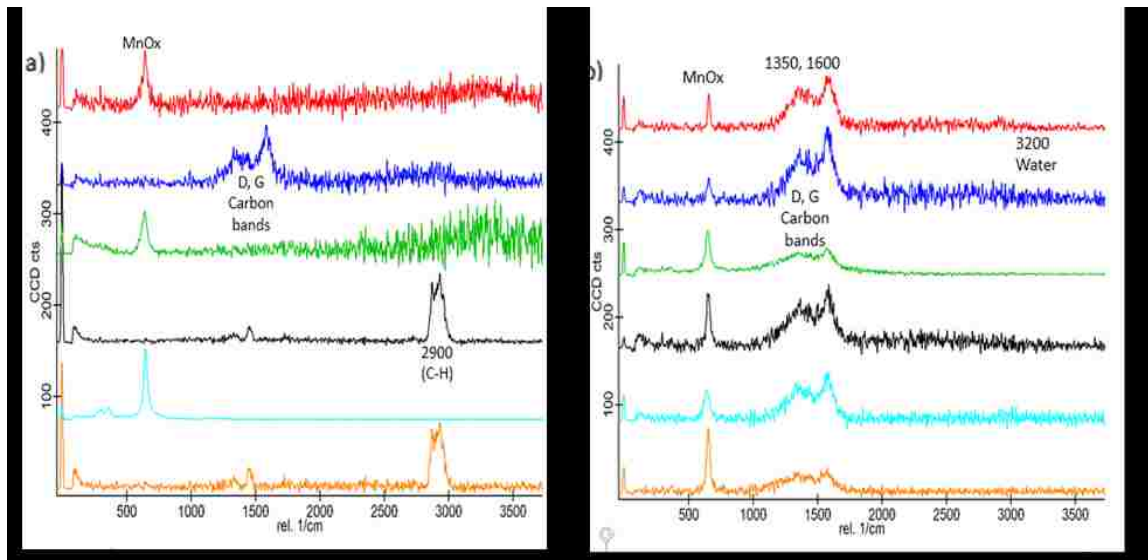
Figure 5. Raman spectra (a) MnO_x Control (unreacted); and (b) MnO_x Phenol samples.
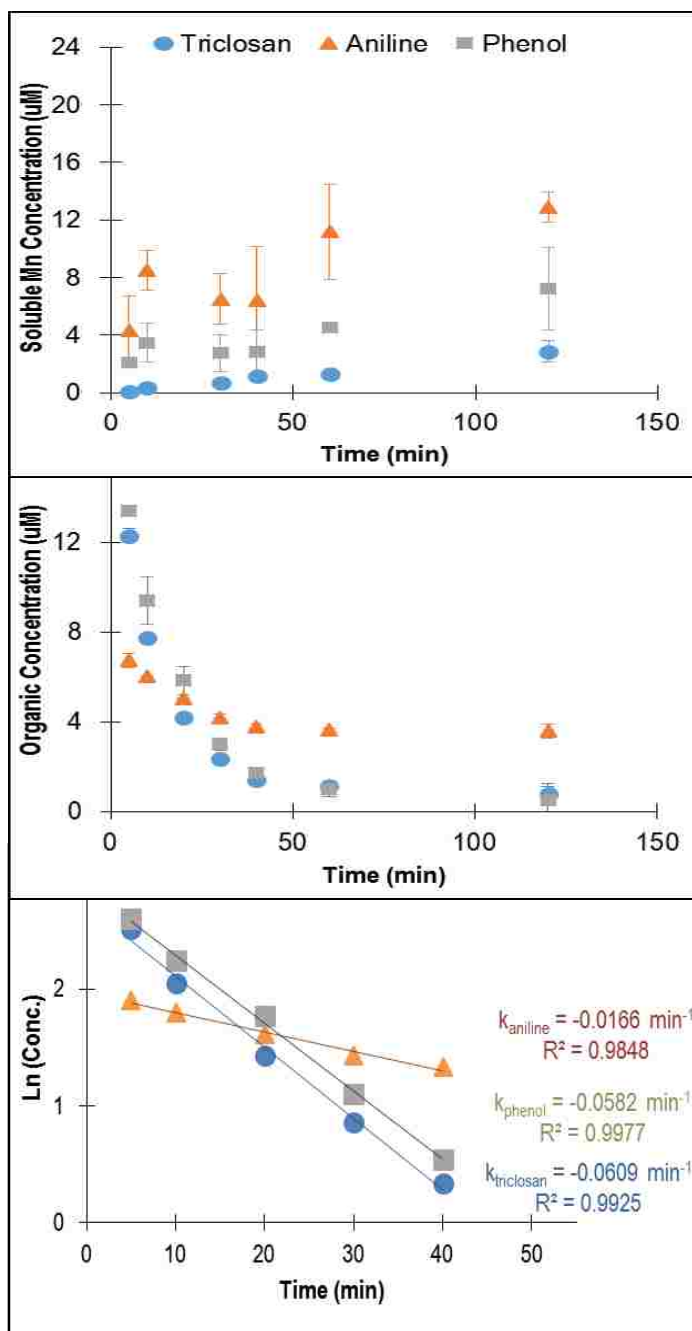
Figure 6. Results from batch reaction experiments conducted with 10 mM MnO_x, 1 mM organic reactant (aniline, phenol, and triclosan), 10 mM NaCl, at pH 5: **a)** Concentrations of Mn released into solution measured with ICP-MS; **b)** Oxidation of triclosan, aniline, and phenol measured with HPLC coupled with DAD. ; and **c)** First order kinetic modelling fits of organic reactants with corresponding k and R^2 values.

Supplementary Information for Spectroscopic Investigation of Interfacial

Interaction of Manganese Oxide with Triclosan, Aniline, and Phenol

Text S1. Synthesis of δ-MnO$_2$. The δ-MnO$_2$ solids used for this study were synthesized using a similar procedure to that followed in previous papers (Taujale et al., 2012). Briefly, in a large beaker, 2L of DI-water were sparged with N$_2$ gas for about 2 hours. From this sparged water, 360 ml was removed and used it for solution preparation by adding: 80 ml 0.1M KMnO$_4$, 160 ml, 0.1M NaOH. Throughout a period of 3 hours, 120 ml of 0.1M MnCl$_2$ were added while the solution was continuously stirred.

Particles of MnO$_x$ particles were allowed to settle. The supernatant was removed and replaced with pure DI-water. Particles were then rinsed by stirring again and allowed to settle. This procedure was repeated until the aqueous supernatant reached a conductivity of less than 2 µS cm^{-1}. The final volume of suspension was adjusted to 1L, resulting in a final concentration of 0.02M MnO$_2$ concentration.

Table S1. Percentage (%) surface carbon bonds composition from C 1s from high resolution spectra fittings.

BE->	284.7	285.6	287.2	288.5
	C-C/C=C	C*-C-Ox	C-OH	C=O
MnOx-Control	49.3	35.9	6.7	8.1
MnOx-Aniline	65.4	23.5	3.6	7.7
MnOx-Phenol	70.0	11.3	12.5	6.1
MnOx-Triclosan	62.1	21.0	14.2	6.6

Table S2. Percentage (%) surface oxygen bonds composition from O 1s from high resolution spectra fitting.

BE->	529.6	531.2	532.5	533.7	535.0
	MnOx	O=N-C/ O=C	C-O-H	C-O-C /COOH	C-O-O-C /H_2O
MnOx-Control	55.5	30.2	10.3	4.0	*BDL*
MnOx-Aniline	50.6	29.7	11.3	8.4	*BDL*
MnOx-Phenol	44.0	21.3	15.9	13.4	5.4
MnOx-Triclosan	48.6	28.4	15.0	8.0	*BDL*

BDL – Below detection limit

Figure S1. Summary of the batch reaction experiment conditions and reactors for this study
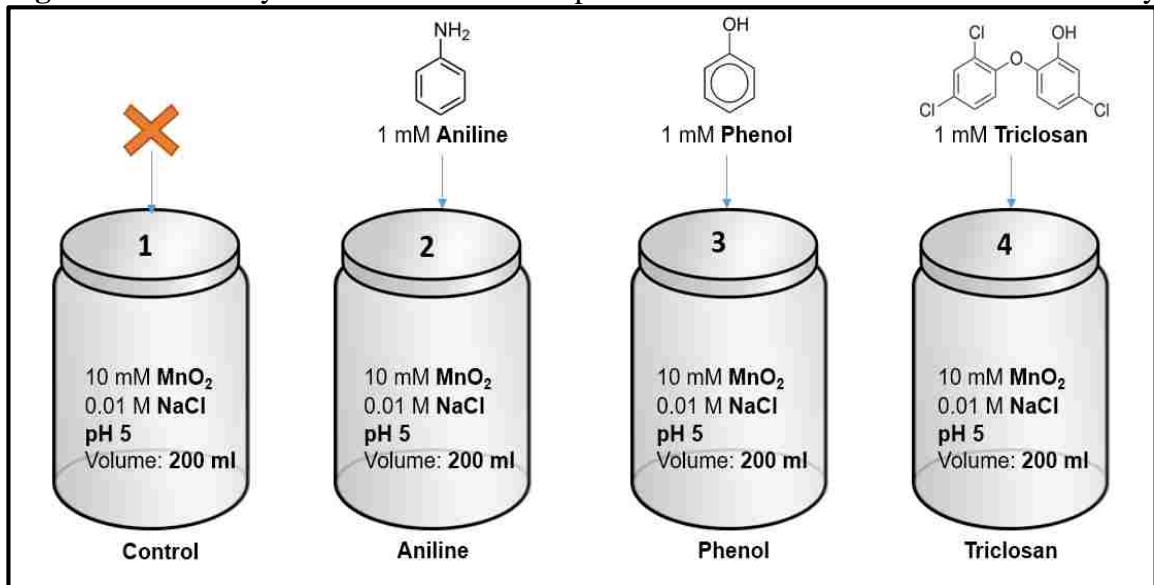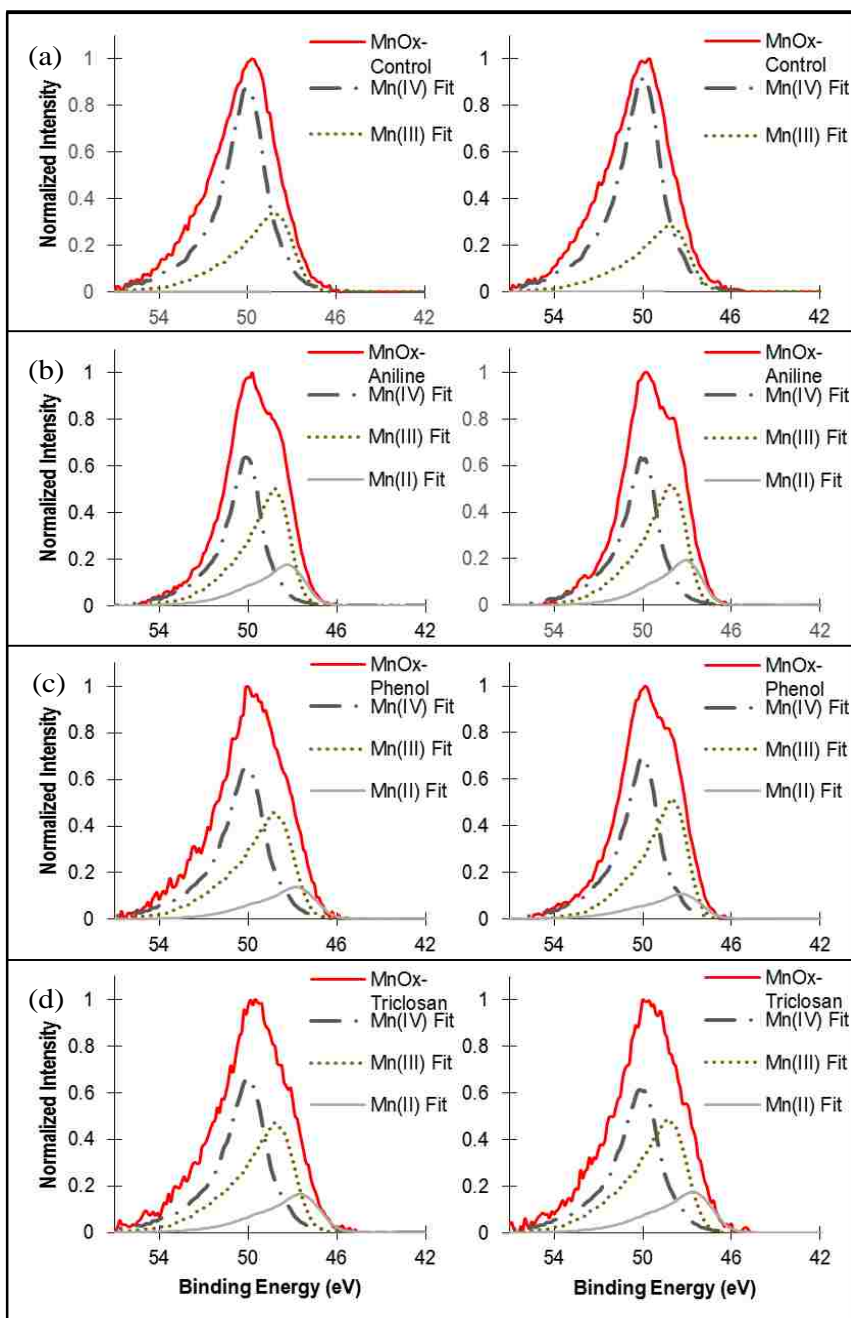
Figure S2. Fitting of XPS high resolution Mn 3p spectra for replicate samples with reference Mn(IV), Mn(III), and Mn(II) spectra for (a) MnO_x Control (b) MnO_x Aniline (c) MnO_x Phenol (d) MnO_x Triclosan samples. The samples are shown in red spectra while the fittings are shown as Mn(IV) component (black dash-dotted line), and Mn(III) component (brown dotted line) and Mn(II) component (grey solid line).

48
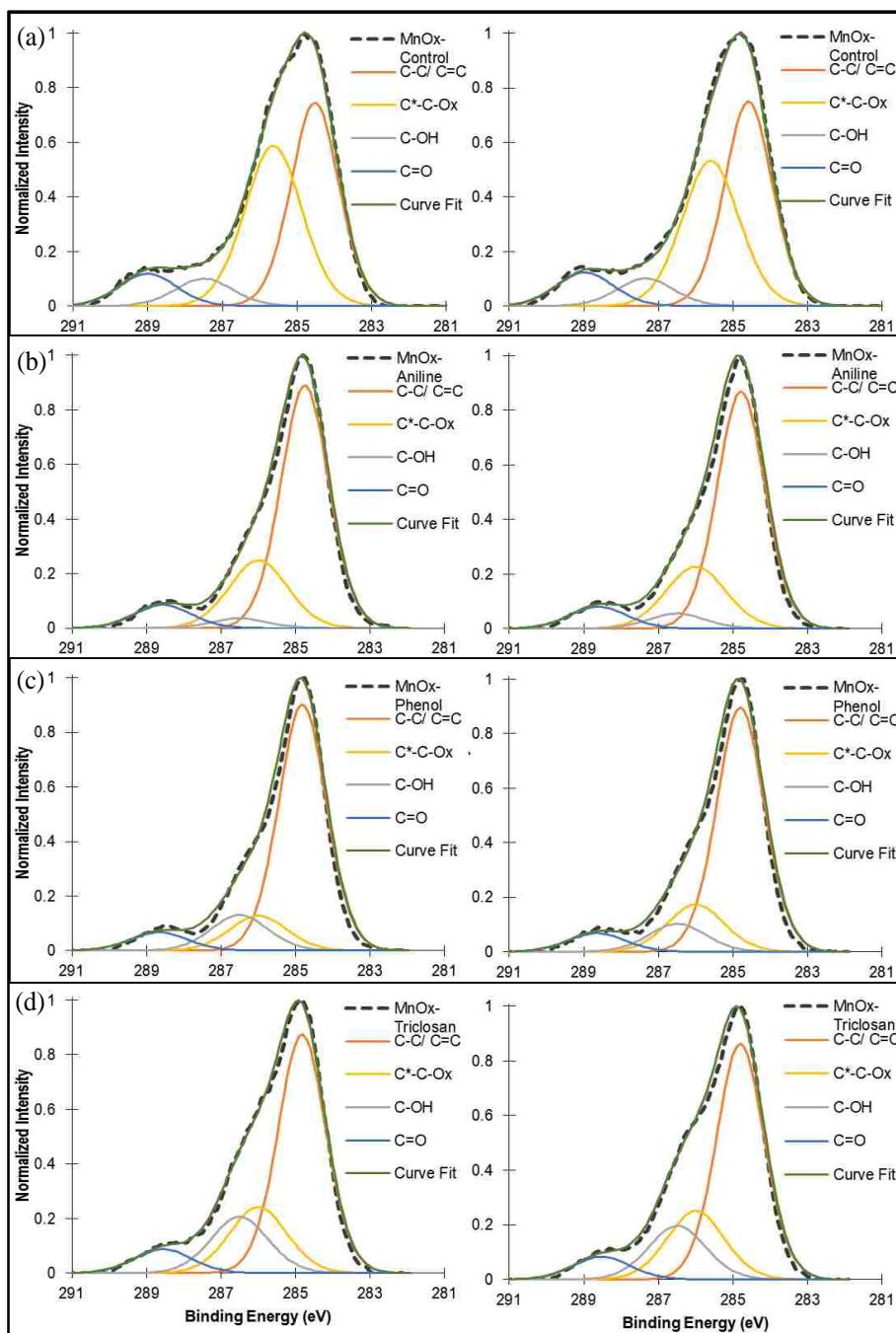
Figure S3. Fitting of C 1s high resolution XPS spectra for replicate samples of (a) MnO$_x$ Control (b) MnO$_x$ Aniline (c) MnO$_x$ Phenol (d) MnO$_x$ Triclosan. The unknown sample data is shown as black dashed line; the solid green line is the overall contribution due to fitting the different types of carbon bonds.

49
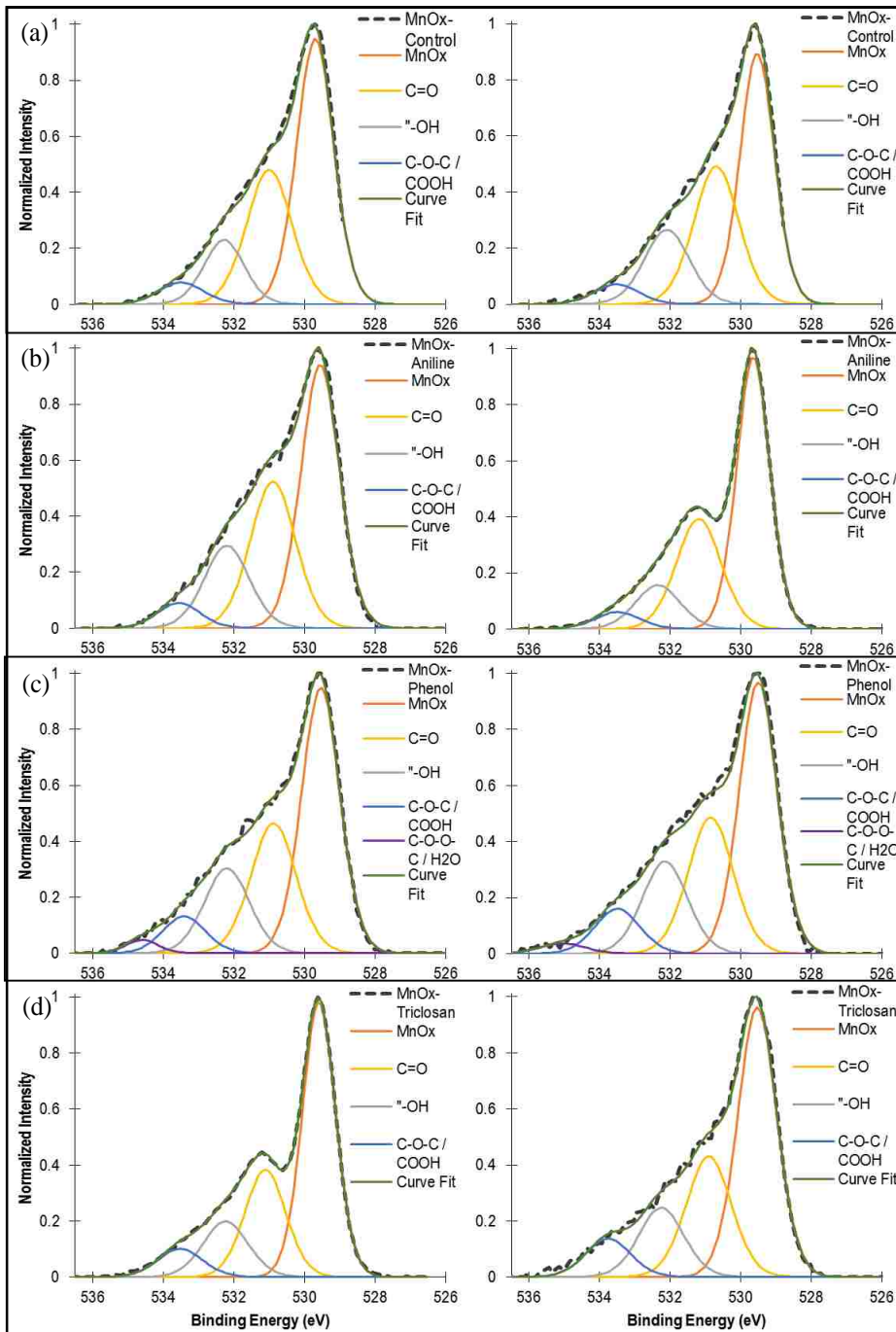
Figure S4. Fitting of O 1s XPS high resolution spectra for replicate samples of (a) MnO_x Control (b) MnO_x Aniline (c) MnO_x Phenol (d) MnO_x Triclosan. The unknown sample data is shown as black dashed line; the solid green line is the overall contribution due to fitting of different types of oxygen bonds.

50
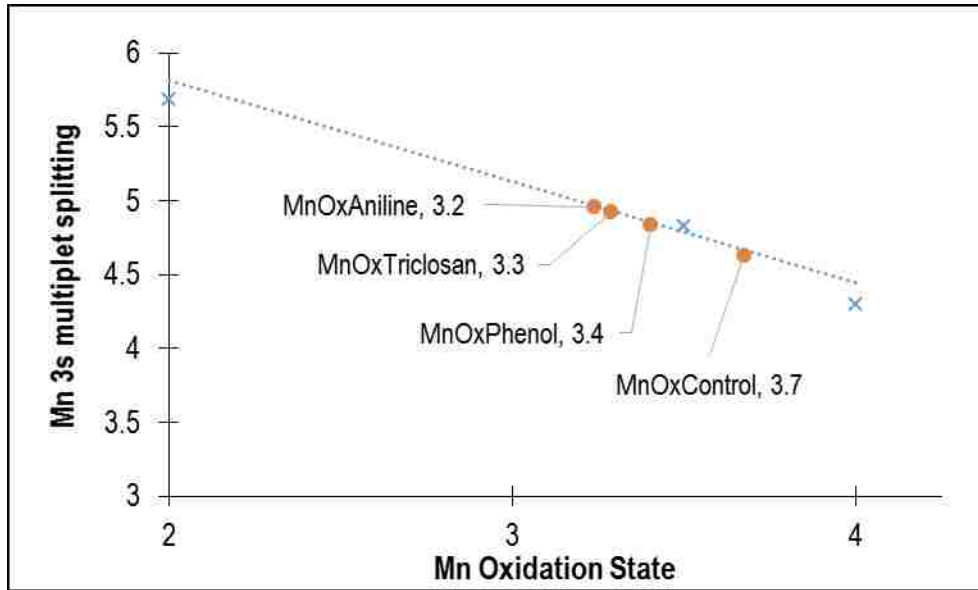
Figure S5. Average oxidation state calculated from Mn 3s multiplet split data for the

reacted and unreacted samples

Preliminary Investigation of the Effect of Surface Area and Metal Impurities on

**$MnO_x(s)$ for the Removal of BPA**

1. Introduction

Bisphenol A (BPA) was widely used as a plasticizer in the polymer production industries and has been found to be estrogenically active with endocrine disruption shown in vivo in uterotrophic assay of BPA exposed immature rats.[92] Structurally similar compounds such as BPF and BPB have also shown disruption.[104] Incomplete removal at current wastewater and drinking water treatment plants has been seen, with the detection of these micropollutants in their effluent streams. Thus, there is a need for effective removal technologies for synthetic organic micropollutants like BPA.

Manganese oxides ($MnO_x(s)$) are some of the most abundant oxides found in soil and sediments. Their redox activity, low point of zero charge and high surface area make them an important part of the bio-geochemical cycle of many compounds, nutrients and contaminants. Mineralogy of MnO_x is varied due to the various oxidation states of Mn, but birnessites are the considered the most common mineral form of MnO_x. Previous studies show that, in laboratory conditions, the organic micropollutants react with MnO_x resulting in reductive dissolution of Mn and oxidation of organic groups. However little is known about the effects of surface area, co-solutes and impurities on MnO_x surface on its reactivity with organic micropollutants. Lin [67] and Lu [81] study the oxidation of BPA and BPF (respectively) by MnO_x with change in pH, humic acid concentration and cations (Ca^{2+}, Mg^{2+}, Mn^{2+}). The potential effects on adsorption, reaction and subsequent release

still needs further exploration. Additionally, most studies utilize synthesized media which are pure and not representative of the manganese oxides present naturally.

The objective of this study was to evaluate the effect of surface area and metal impurities on commercially available MnO_x for the removal of BPA using spectroscopy and aqueous chemistry techniques. A secondary objective was to investigate changes in Mn oxidation of $MnO_x(s)$ and interactions at the solid-water interface with BPA using X-ray photoelectron spectroscopy (XPS). Synthetic (with limited impurities) and commercially available $MnO_x(s)$ with different surface areas were used to perform this research which provides relevant insights about the applicability of these $MnO_x(s)$ for treatment of organic micropollutants. Additionally, the results from this study are relevant to better understand chemical interactions of $MnO_x(s)$ and organic compounds in natural and engineered systems.

2. Materials and Methods

2.1. Materials.

Bisphenol A (>99% purity) was purchased from Sigma Aldrich (St. Louis, MO). Commercial $MnO_x(s)$ (Com-MnO_x) (purchased from Layne Co., TX) is a $MnO_x(s)$ filter media, which is used to remove inorganics from drinking water. Pure (>99%) manganese oxides (MnO, Mn_2O_3, MnO_2 and Mn (III,IV) oxide) were purchased from Strem Chemicals (Newburyport, MA) and Sigma Aldrich (St. Louis, MO). All other chemicals where bought from VWR or Thermo Fisher with >90% purity and used without further purification. Delta manganese dioxide (δ-MnO_x) was used in this study, as it is considered analogous to birnessite.[42,43] Birnessite is the naturally abundant form of manganese oxide and

53

structurally arranged as edge sharing MnO_6 octahedra with mixed valent manganese centers.[53] The δ-MnO_x (Syn-MnO_x) was synthesized as done by Taujale and Zhang [79] reacting $KMnO_4$ and $MnCl_2$ in basic conditions.

2.2. Batch Experiments.

Bisphenol A reaction with $MnO_x(s)$ was studied to examine the impacts of solutes and impurities on the net release of manganese into solution and degradation of BPA. First, batch experiments were conducted with 1mM BPA reacting with 10mM Syn-MnO_x or 10mM Com-MnO_x (in separate reactors) in ultrapure water at pH 5.5 (phosphate buffer). 0.01mM NaCl was added to the reactors to maintain ionic strength. The pH 5.5 was chosen to keep the study at relevant pH to natural and engineered systems while being low enough for the reaction to be appreciably completed within the experimental time-frame. Liquid samples, 10 ml filtered through 0.45 microns, were taken at timed intervals (5, 15, 30, 45, 90, 180 mins and 2 days) to evaluate the dissolved Mn and BPA residual.

2.3. Adsorption Experiments.

The reactors for kinetic experiments were set up in 60 ml screw-cap amber bottles with Teflon caps. Reactors were placed on magnetic stir plates and stirred continuously at 22±3 °C. 25 mM acetate buffer was added to adjust pH of reactors to 5.0 (±0.1). In order to obtain constant ionic strength, 0.01 M NaCl was added to the reactors. The concentration of Syn-MnO_x or Com-MnO_x in the reactors was 100 µM. 50 µl of BPA stock solution (10 µM) was added to the reactors to initiate the reaction. The reaction course at these different time points were monitored by following two different approaches to quench kinetic reactions. First, the reaction aliquots were collected in clean centrifuge tubes, centrifuged

54

at 13400 rpm for 15 minutes, filtered into HPLC vials for analysis. Second, reaction aliquots were collected in centrifuge tubes that contained NaOH in order to increase pH to 10.0, centrifuged and filtered.

3. Results and Discussion

3.1. BPA Removal

The removal of BPA by different $MnO_x(s)$ media was assessed. **Figure S6** illustrates the data for residual BPA concentrations over time. As expected, the control samples for both Com-MnO_x and Syn-MnO_x showed no BPA concentrations, and BPA remained stable in absence of $MnO_x(s)$ under the employed experimental conditions. The reacted samples showed rapid BPA removal initially, with 67% and 61% of BPA removed in first 15 mins for Syn-MnO_x and Com-MnO_x respectively. As the reaction proceeds from 15 mins onwards, BPA removal followed first order kinetics with rates of 1.1 hr-1 and 0.0056 hr-1 and removal efficiency of 99.8% and 71% for Syn-MnO_x and Com-MnO_x respectively. The removal was likely caused by adsorption and oxidation of BPA on MnO_x media as reported in other studies.[26,67] The rapid initial removal can be attributed to rapid oxidation of BPA on the available surface sites. The oxidation rate is the limiting step in this phase of reaction. As the reaction proceeds, the surface sites get occupied irreversibly by oxidation products and reduced Mn, resulting in adsorption being the rate limiting step. Thus we see 2 distinct phases of BPA removal rates.

The data from the adsorption experiment show that similar overall BPA removal efficacy of 95% and 75% for Syn-MnO_x and Com-MnO_x respectively. **Figure S7** shows that BPA removal was mainly due to oxidation in case of Com-MnO_x, while Syn-MnO_x had retained

55

un-oxidized BPA on its surface, which was released by an increase in pH by addition of excess NaOH. MnO_x has a high sorption capability, with sorbed BPA and redox products occupying the surface sites, resulting in surface passivation as the reaction proceeds. The amount of BPA removed by sorption also followed first order kinetics with maximum adsorbed BPA on MnO_x at 34 μM BPA / mM MnO_x for Syn-MnO_x, and 3.3 μM BPA / mM MnO_x for Com-MnO_x. This difference can be attributed to the lower surface area of Com-MnO_x (13.8 m^2/g) compared to Syn-MnO_x (128.3 m^2/g).

3.2. Soluble Mn Release to Solution

The liquid samples from the reactor taken at timed intervals; results are illustrated in **Figure S8**. The Syn-MnO_x media reacted with BPA showed exponentially increasing release of Mn, with final value of 14 mg/l after 2 days. Com-MnO_x reacted sample, showed a rapid increase, but not to the scale of Syn-MnO_x, with the final value of 1.1 mg/l after 2 days of reaction. This increasing presence of Mn in reactor and data from solid analysis suggests towards reductive dissolution of Mn in MnO_x media. The variation of Mn release for the two media is proportional to the surface area of the media, with an order of magnitude difference in surface areas and Mn in solution respectively. Thus, these data suggest that the amount of available surface binding sites is the rate limiting step for oxidation of BPA and, subsequently, for re-sorption/re-oxidation of aqueous Mn onto MnO_x as suggested in other studies.[29,97,98]

3.3. Surface Area, Elemental Composition, and Structure of MnO_x(s)

The surface area from BET was 13.6 m^2/g for Com-MnO_x and 128.3 m^2/g for Syn-MnO_x. The X-ray diffractogram) showed that the MnO_x was poorly crystalline with structural

56

similarities to birnessite and todorokite. **Table S3** shows the bulk elemental composition of Com-MnO$_x$ and Syn-MnO$_x$ media. Al (10%), Fe (9 %) and Si (7%) are the most abundant impurities in the Com-MnO$_x$ media, Mn content was at 71%. The Syn-MnO$_x$ did not show any other metal impurities and thus considered pure δ-MnO$_x$.

3.3.1. Near Surface Elemental Composition

The survey scan of the top 5-10 nm (near surface) using the XPS was carried out for the unreacted (control) and BPA-reacted media (Com-MnO$_x$ and Syn-MnO$_x$) to quantify the surface elemental composition. The carbon content (C 1s) for control Com-MnO$_x$ was 46.8% and for control Syn-MnO$_x$ was 38.8%, likely due to the contribution of adventitious carbon. In contrast, there was an increase in C 1s for both reacted Com-MnO$_x$ and reacted Syn-MnO$_x$ with 60.9% and 60.4% respectively, suggesting the possible association of organic compounds to the MnO$_x$ surface. Since the MnO$_x$ samples were collected to be analyzed after the reaction had been sufficiently completed, the parent compound (BPA) has been mostly oxidized, with oxidation products remaining associated to the MnO$_x$ surface. The scan of the control and reacted Com-MnO$_x$ samples shows the presence of Al and Si in the surface confirming the presence of impurities in Com-MnO$_x$. A decrease in Al in the surface of reacted Com-MnO$_x$ samples (2.8%) compared to 5.1% in control Com-MnO$_x$ samples was observed, while the Si content showed a slight decrease in reacted Com-MnO$_x$ samples (3.2%) when compared to 3.7% in control Com-MnO$_x$ samples. A significant decrease in Mn is seen in Syn-MnO$_x$, from 11.7% in control Syn-MnO$_x$ samples to 6.2% for the reacted Syn-MnO$_x$ samples. The Mn content in control Com-MnO$_x$ sample 1.9% showed a slight decrease when reacted with BPA, reacted Com-MnO$_x$ samples at

57

1.4%. Additional analysis on narrow scans of the Mn 3s and Mn 3p spectra was carried out to investigate the Mn oxidation state.

3.3.2. Oxidation State of Mn in $MnO_x(s)$

A similar method to that presented in Chapter 3 was used to determine Mn oxidation states in this appendix. Mn 3s multiplet splitting, which is a feasible method for determining Mn oxidation,[36,83] was obtained from XPS narrow scan on the control and reacted samples, and the reference materials for Mn (IV), Mn (III) and Mn (II) oxides (**Table S4**). The data shows an increase in splitting values for reacted Syn-MnO_x (4.82) compared to 4.63 for control Syn-MnO_x, and similar increase for reacted Com-MnO_x (4.68) compared to 4.47 for control Com-MnO_x. Correlating the values to reference Mn data, the value of 4.82 for reacted Syn-MnO_x is within 0.08 eV of the Mn(III, IV) reference and the value of 4.47 for control Com-MnO_x is within 0.09 eV of the Mn(IV) reference. The increase in multiplet splitting for reacted samples suggests reduction in Mn oxidation state. On comparison with Mn reference data, the average surface Mn oxidation state for control Syn-MnO_x was 3.7 and control Com-MnO_x was 3.8, consistent with data from other studies of 3.6 to 3.8 for unreacted birnessite.[29,53,102]. The average Mn oxidation state for reacted Syn-MnO_x was 3.5 and for reacted Com-MnO_x was 3.6 which indicated reduction of Mn on the surface. In spite of the impurities on surface of Com-MnO_x, it had a higher Mn oxidation state for both control and reacted samples compared to Syn-MnO_x.

4. Conclusions

a) Release of Mn was proportional to surface area available. However, BPA removal was not proportional to surface area.

58

b) Impurities on $MnO_x(s)$ surface such as Al and Silicon oxides decrease the BPA removal efficiency, but also reduces Mn dissolution by occupying surface sites.

c) An increase Mn (III) and Mn (II) was detected in the surface of MnOx(s) using XPS analyses, suggesting that Mn in the surface was reduced when reacted with BPA and reduced species are associated to the $MnO_x(s)$ surface. Future research should determine if reduced Mn(III) and Mn(II) is adsorbed and/or incorporated to the solid $MnO_x(s)$.

59

Table S3. Summary of characteristic of MnO_x media used in this study. [a] Multipoint – N_2 BET; [b] data from X-ray Fluorescence (XRF); [c] data from SEM/EDS

	Com-MnO_x	Syn-MnO_x
Specific surface area (m^2/g) [a]	13.6	128.3
Elemental composition (%)		
Manganese	71.2 [b]	99.9 [c]
Aluminum	9.65 [b]	-
Iron	8.97 [b]	-
Silicon	6.88 [b]	-
Potassium	1.34 [b]	-
Titanium	0.425 [b]	-
Barium	0.367 [b]	-
Calcium	0.302 [b]	-

Table S4. Mn 3s multiplet splitting results for a) Reference Mn oxides and b) control and reacted samples. Curve 1 and curve 2 corresponds to the position/binding energy of ^5S and ^7S for each sample.

	Sample	Curve 1: Mn ^5S (eV)	Curve 2: Mn ^7S (eV)	Multiplet Splitting (eV)
a)	MnO; Mn(II)	89.10	83.40	5.69
References	Mn_2O_3; Mn(III)	88.52	83.20	5.33
	Li Mn(III,IV)O	88.94	84.05	4.90
	MnO_2; Mn(IV)	88.89	84.52	4.38
b)	Syn-MnO_x Control	89.40	84.77	4.63
Samples	Syn-MnO_x Reacted	89.27	84.45	4.82
	Com-MnO_x Control	87.04	82.57	4.47
	Com-MnO_x Reacted	87.93	83.25	4.68

61
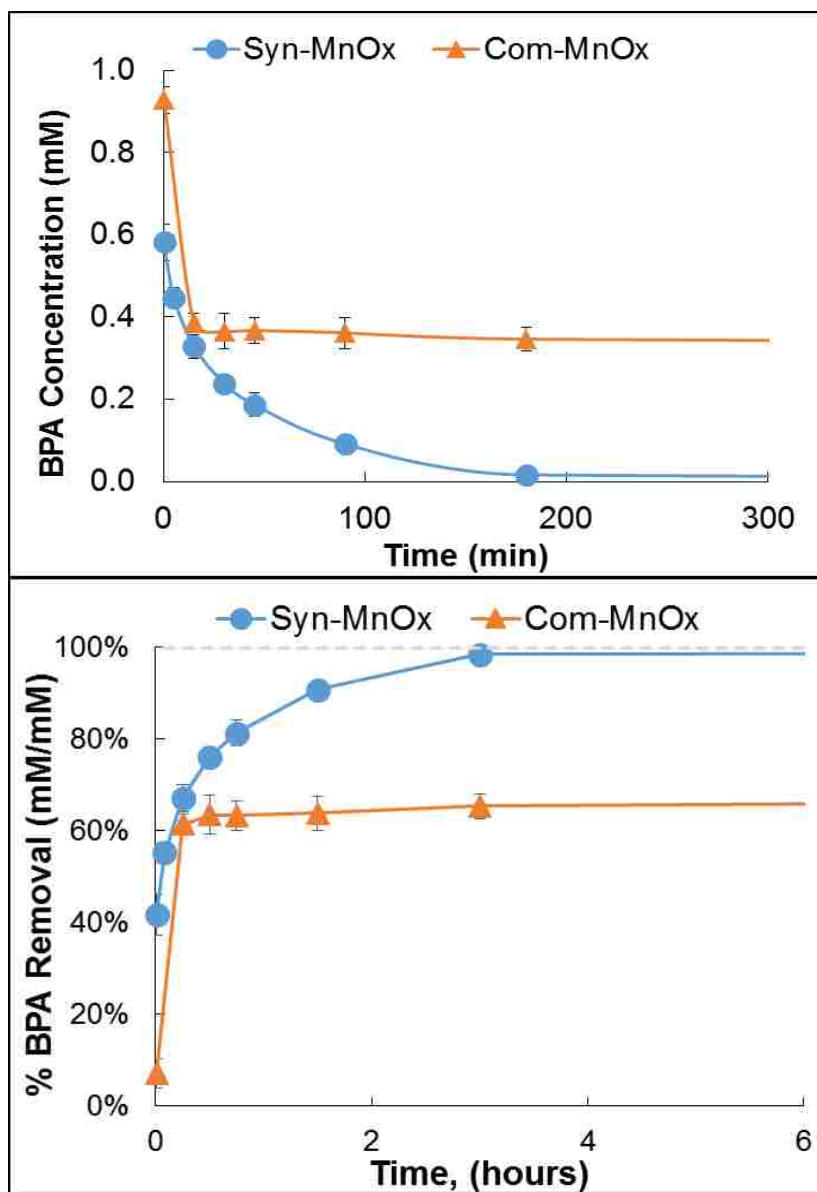
Figure S6. HPLC-ECD data for residual BPA in aliquots from batch experiments (n=2) of solutions reacted with Commercial MnO_x and Synthesized $MnO_x(s)$ taken at t= 0.1, 5, 15, 30, 45, 90, 180 and 2640 mins. Reaction conditions were 10 mM MnO_x, 1 mM BPA, 10 mM NaCl and pH 5.5.
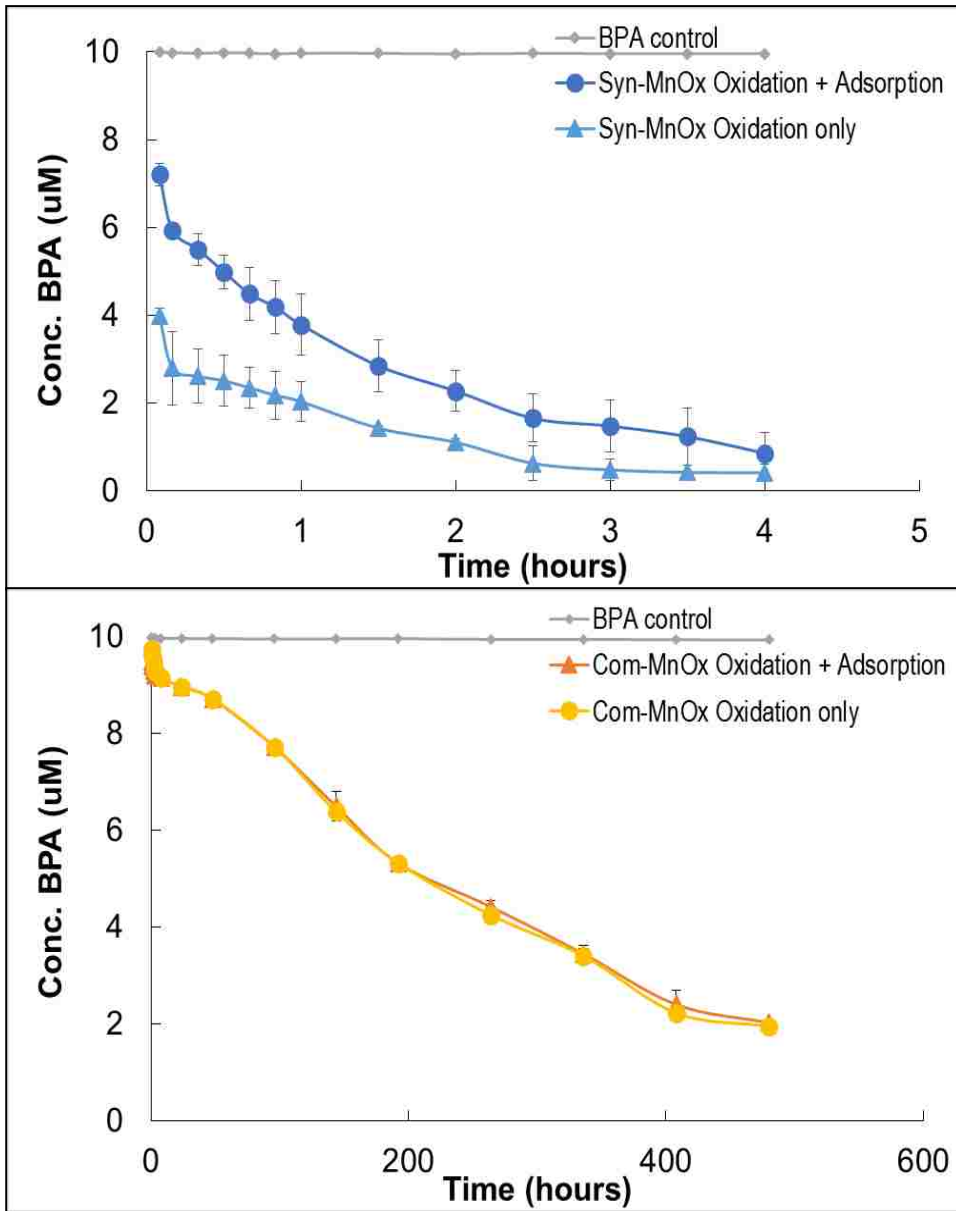
Figure S7. BPA removed by oxidation and adsorption vs. BPA removed by oxidation alone. Reaction conditions: 100 μM MnO_x, 10 μM BPA, 10 mM NaCl, pH 5.0

63
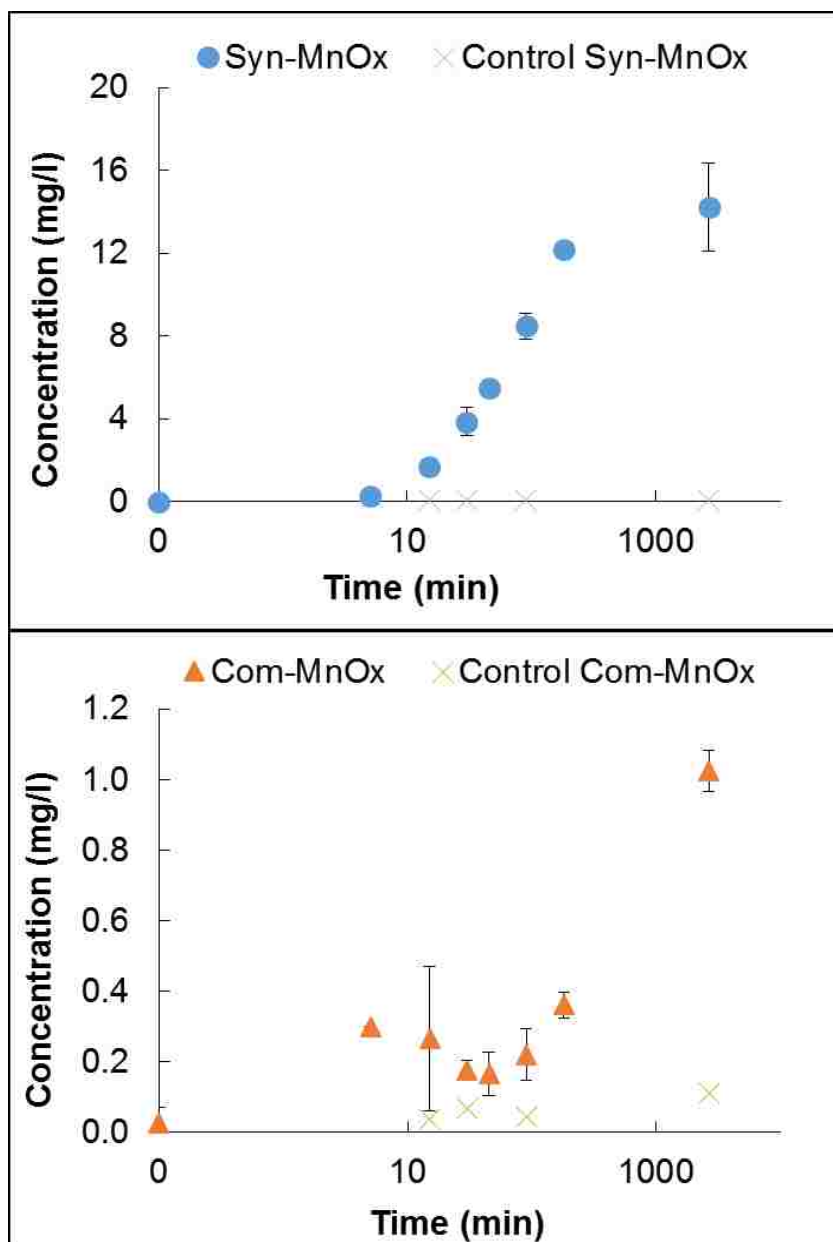
Figure S8. ICP-MS data for Mn release into solution from batch experiments (n=4) for a) Synthesized MnO_x and b) Commercial MnO_x for reacted samples taken at t= 5, 15, 30, 45, 90, 180 and 2640 mins. Reaction conditions were 10 mM MnO_x, 1 mM BPA, 10 mM NaCl and pH 5.5. The crosses represents MnO_x reactors without any BPA.

64

References

(1)   Sedlak, D. L.; Schnoor, J. L. The Challenge of Water Sustainability. *Environ. Sci. Technol.* **2013**, *47* (11), 5517–5517.

(2)   Snyder, S. A.; Westerhoff, P.; Yoon, Y.; Sedlak, D. L. Pharmaceuticals, Personal Care Products, and Endocrine Disruptors in Water: Implications for the Water Industry. *Environ. Eng. Sci.* **2003**, *20* (5), 449–469.

(3)   Oulton, R. L.; Kohn, T.; Cwiertny, D. M. Pharmaceuticals and personal care products in effluent matrices: a survey of transformation and removal during wastewater treatment and implications for wastewater management. *J. Environ. Monit.* **2010**, *12*, 1956–1978.

(4)   Backe, W. J.; Ort, C.; Brewer, A. J.; Field, J. A. Analysis of Androgenic Steroids in Environmental Waters by Large-Volume Injection Liquid Chromatography Tandem Mass Spectrometry. *Anal. Chem.* **2011**, *83* (7), 2622–2630.

(5)   Kolpin, D. W.; Furlong, E. T.; Meyer, M. T.; Thurman, E. M.; Zaugg, S. D.; Barber, L. B.; Buxton, H. T. Pharmaceuticals, Hormones, and Other Organic Wastewater Contaminants in U.S. Streams, 1999−2000: A National Reconnaissance. *Environ. Sci. Technol.* **2002**, *36* (6), 1202–1211.

(6)   Thorpe, K. L.; Hutchinson, T. H.; Hetheridge, M. J.; Scholze, M.; Sumpter, J. P.; Tyler, C. R. Assessing the Biological Potency of Binary Mixtures of Environmental Estrogens using Vitellogenin Induction in Juvenile Rainbow Trout (Oncorhynchus mykiss). *Environ. Sci. Technol.* **2001**, *35* (12), 2476–2481.

(7)   Chalew, T. E. A.; Halden, R. U. Environmental Exposure of Aquatic and Terrestrial Biota to Triclosan and Triclocarban1. *JAWRA J. Am. Water Resour. Assoc.* **2009**, *45* (1), 4–13.

(8)   Schmitt, C. J.; Ellen Hinck, J.; Blazer, V. S.; Denslow, N. D.; Dethloff, G. M.; Bartish, T. M.; Coyle, J. J.; Tillitt, D. E. Environmental contaminants and biomarker responses in fish from the Rio Grande and its U.S. tributaries: Spatial and temporal trends. *Sci. Total Environ.* **2005**, *350*, 161–193.

(9)   Hinck, J. E.; Blazer, V. S.; Schmitt, C. J.; Papoulias, D. M.; Tillitt, D. E. Widespread occurrence of intersex in black basses (Micropterus spp.) from U.S. rivers, 1995–2004. *Aquat. Toxicol.* **2009**, *95* (1), 60–70.

(10)   Zhang, T. C.; Emary, S. C. Jar Tests for Evaluation of Atrazine Removal at Drinking Water Treatment Plants. *Environ. Eng. Sci.* **1999**, *16* (6), 417–432.

(11)   Westerhoff, P.; Yoon, Y.; Snyder, S.; Wert, E. Fate of Endocrine-Disruptor, Pharmaceutical, and Personal Care Product Chemicals during Simulated Drinking Water Treatment Processes. *Environ. Sci. Technol.* **2005**, *39* (17), 6649–6663.

(12)   Mitch, W. A.; Sedlak, D. L. Characterization and Fate of N-Nitrosodimethylamine Precursors in Municipal Wastewater Treatment Plants. *Environ. Sci. Technol.* **2004**, *38* (5), 1445–1454.

(13)   Huber, M. M.; Canonica, S.; Park, G.-Y.; von Gunten, U. Oxidation of Pharmaceuticals during Ozonation and Advanced Oxidation Processes. *Environ. Sci. Technol.* **2003**, *37* (5), 1016–1024.

(14)   von Gunten, U. Ozonation of drinking water: Part I. Oxidation kinetics and product formation. *Water Res.* **2003**, *37* (7), 1443–1467.

(15)   von Gunten, U. Ozonation of drinking water: Part II. Disinfection and by-product formation in presence of bromide, iodide or chlorine. *Water Res.* **2003**, *37* (7), 1469–1487.

(16) He, D.; Guan, X.; Ma, J.; Yang, X.; Cui, C. Influence of humic acids of different origins on oxidation of phenol and chlorophenols by permanganate. *J. Hazard. Mater.* **2010**, *182* (1–3), 681–688.

(17) Scott, M. J.; Morgan, J. J. Reactions at Oxide Surfaces. 1. Oxidation of As(III) by Synthetic Birnessite. *Environ. Sci. Technol.* **1995**, *29* (8), 1898–1905.

(18) Sherman, D. M.; Peacock, C. L. Surface complexation of Cu on birnessite (delta-MnO2): Controls on Cu in the deep ocean. *Geochim. Cosmochim. Acta* **2010**, *74*, 6721–6730.

(19) Xyla, A. G.; Sulzberger, B.; Luther, G. W.; Hering, J. G.; Van Cappellen, P.; Stumm, W. Reductive dissolution of manganese(III, IV) (hydr)oxides by oxalate: the effect of pH and light. *Langmuir* **1992**, *8* (1), 95–103.

(20) Trouwborst, R. E.; Clement, B. G.; Tebo, B. M.; Glazer, B. T.; Luther, G. W. Soluble Mn(III) in Suboxic Zones. *Science* **2006**, *313* (5795), 1955–1957.

(21) Kim, J.; Dixon, J.; Chusuei, C.; Deng, Y. Oxidation of chromium(III) to (VI) by manganese oxides. *Fac. Res. Creat. Works* **2002**.

(22) Friedl, G.; Wehrli, B.; Manceau, A. Solid phases in the cycling of manganese in eutrophic lakes: New insights from EXAFS spectroscopy. *Geochim. Cosmochim. Acta* **1997**, *61* (2), 275–290.

(23) Nico, P. S.; Zasoski, R. J. Importance of Mn(III) Availability on the Rate of Cr(III) Oxidation on δ-MnO2. *Environ. Sci. Technol.* **2000**, *34* (16), 3363–3367.

(24) Wang, Z.; Lee, S.-W.; Kapoor, P.; Tebo, B. M.; Giammar, D. E. Uraninite oxidation and dissolution induced by manganese oxide: A redox reaction between two insoluble minerals. *Geochim. Cosmochim. Acta* **2013**, *100*, 24–40.

(25) Zhang, H.; Chen, W.-R.; Huang, C.-H. Kinetic Modeling of Oxidation of Antibacterial Agents by Manganese Oxide. *Environ. Sci. Technol.* **2008**, *42* (15), 5548–5554.

(26) Remucal, C. K.; Ginder-Vogel, M. A critical review of the reactivity of manganese oxides with organic contaminants. *Environ. Sci. Process. Impacts* **2014**, *16* (6), 1247–1266.

(27) Xu, L.; Xu, C.; Zhao, M.; Qiu, Y.; Sheng, G. D. Oxidative removal of aqueous steroid estrogens by manganese oxides. *Water Res.* **2008**, *42*, 5038–5044.

(28) Laha, S.; Luthy, R. G. Oxidation of aniline and other primary aromatic amines by manganese dioxide. *Environ. Sci. Technol.* **1990**, *24* (3), 363–373.

(29) Stone, A. T. Reductive Dissolution of Manganese(III/IV) Oxides by Substituted Phenols. *Environ. Sci. Technol.* **1987**, *21* (10), 979–988.

(30) Jiang, J.; Gao, Y.; Pang, S.-Y.; Lu, X.-T.; Zhou, Y.; Ma, J.; Wang, Q. Understanding the Role of Manganese Dioxide in the Oxidation of Phenolic Compounds by Aqueous Permanganate. *Environ. Sci. Technol.* **2015**, *49* (1), 520–528.

(31) Zhang, H.; Huang, C.-H. Oxidative Transformation of Triclosan and Chlorophene by Manganese Oxides. *Environ. Sci. Technol.* **2003**, *37* (11), 2421–2430.

(32) Zhang, H.; Taujale, S.; Huang, J.; Lee, G.-J. Effects of NOM on Oxidative Reactivity of Manganese Dioxide in Binary Oxide Mixtures with Goethite or Hematite. *Langmuir* **2015**, *31* (9), 2790–2799.

(33) Tipping, E.; Heaton, M. J. The adsorption of aquatic humic substances by two oxides of manganese. *Geochim. Cosmochim. Acta* **1983**, *47* (8), 1393–1397.

(34) Klausen, J.; Haderlein, S. B.; Schwarzenbach, R. P. Oxidation of Substituted Anilines by Aqueous MnO2: Effect of Co-Solutes on Initial and Quasi-Steady-State Kinetics. *Environ. Sci. Technol.* **1997**, *31* (9), 2642–2649.

(35) Luther III, G. W. Manganese(II) Oxidation and Mn(IV) Reduction in the Environment—Two One-Electron Transfer Steps Versus a Single Two-Electron Step. *Geomicrobiol. J.* **2005**, *22* (3-4), 195–203.

(36) Cerrato, J. M.; Knocke, W. R.; Hochella, M. F.; Dietrich, A. M.; Jones, A.; Cromer, T. F. Application of XPS and Solution Chemistry Analyses to Investigate Soluble Manganese Removal by MnOx(s)-Coated Media. *Environ. Sci. Technol.* **2011**, *45*, 10068–10074.

(37) Appelo, C. A. J.; Postma, D. A consistent model for surface complexation on birnessite (−MnO2) and its application to a column experiment. *Geochim. Cosmochim. Acta* **1999**, *63* (19–20), 3039–3048.

(38) Peter B. Merkle, W. K. Characterizing filter media mineral coatings. *J. Am. Water Works Assoc. - J AMER WATER WORK ASSN* **1996**, *88* (12), 62–73.

(39) Post, J. E. Manganese oxide minerals: Crystal structures and economic and environmental significance. *Proc. Natl. Acad. Sci.* **1999**, *96* (7), 3447–3454.

(40) Webb, S. M.; Tebo, B. M.; Barger, J. R. Structural Influences of Sodium and Calcium Ions on the Biogenic Manganese Oxides Produced by the Marine Bacillus Sp., Strain SG-1. *Geomicrobiol. J.* **2005**, *22* (3-4), 181–193.

(41) Turner, S.; Buseck, P. R. Todorokites: A New Family of Naturally Occurring Manganese Oxides. *Science* **1981**, *212* (4498), 1024–1027.

(42) Villalobos, M.; Toner, B.; Bargar, J.; Sposito, G. Characterization of the manganese oxide produced by pseudomonas putida strain MnB1. *Geochim. Cosmochim. Acta* **2003**, *67* (14), 2649–2662.

(43) Webb, S. M.; Tebo, B. M.; Bargar, J. R. Structural characterization of biogenic Mn oxides produced in seawater by the marine bacillus sp. strain SG-1. *Am. Mineral.* **2005**, *90* (8-9), 1342–1357.

(44) Tebo, B. M.; Bargar, J. R.; Clement, B. G.; Dick, G. J.; Murray, K. J.; Parker, D.; Verity, R.; Webb, S. M. BIOGENIC MANGANESE OXIDES: Properties and Mechanisms of Formation. *Annu. Rev. Earth Planet. Sci.* **2004**, *32* (1), 287–328.

(45) Webb, S. M.; Fuller, C. C.; Tebo, B. M.; Bargar, J. R. Determination of Uranyl Incorporation into Biogenic Manganese Oxides Using X-ray Absorption Spectroscopy and Scattering. *Environ. Sci. Technol.* **2006**, *40* (3), 771–777.

(46) Alessi, D. S.; Lezama-Pacheco, J. S.; Janot, N.; Suvorova, E. I.; Cerrato, J. M.; Giammar, D. E.; Davis, J. A.; Fox, P. M.; Williams, K. H.; Long, P. E.; et al. Speciation and Reactivity of Uranium Products Formed during in Situ Bioremediation in a Shallow Alluvial Aquifer. *Environ. Sci. Technol.* **2014**, *48* (21), 12842–12850.

(47) Lafferty, B. J.; Ginder-Vogel, M.; Sparks, D. L. Arsenite Oxidation by a Poorly Crystalline Manganese-Oxide 1. Stirred-Flow Experiments. *Environ. Sci. Technol.* **2010**, *44* (22), 8460–8466.

(48) Fendorf, S. E.; Zasoski, R. J. Chromium(III) oxidation by .delta.-manganese oxide (MnO2). 1. Characterization. *ChromiumIII Oxid. Delta-Manganese Oxide MnO2 1 Charact.* **1992**, *26* (1), 79–85.

(49) Luther III, G. W.; Sundby, B.; Lewis, B. L.; Brendel, P. J.; Silverberg, N. Interactions of manganese with the nitrogen cycle: Alternative pathways to dinitrogen. *Geochim. Cosmochim. Acta* **1997**, *61* (19), 4043–4052.

(50) Tebo, B. M.; Johnson, H. A.; McCarthy, J. K.; Templeton, A. S. Geomicrobiology of manganese(II) oxidation. *Trends Microbiol.* **2005**, *13* (9), 421–428.

67

(51) Webb, S. M.; Dick, G. J.; Bargar, J. R.; Tebo, B. M. Evidence for the presence of Mn(III) intermediates in the bacterial oxidation of Mn(II). *Proc. Natl. Acad. Sci. U. S. A.* **2005**, *102* (15), 5558–5563.

(52) Kostka, J. E.; Luther III, G. W.; Nealson, K. H. Chemical and biological reduction of Mn (III)-pyrophosphate complexes: Potential importance of dissolved Mn (III) as an environmental oxidant. *Geochim. Cosmochim. Acta* **1995**, *59* (5), 885–894.

(53) Nico, P. S.; Zasoski, R. J. Mn(III) Center Availability as a Rate Controlling Factor in the Oxidation of Phenol and Sulfide on δ-MnO2. *Environ. Sci. Technol.* **2001**, *35* (16), 3338–3343.

(54) Nesbitt, H. W.; Banerjee, D. Interpretation of XPS Mn(2p) spectra of Mn oxyhydroxides and constraints on the mechanism of MnO 2 precipitation. *Am. Mineral.* **1998**, *83* (3-4), 305–315.

(55) Krishnan, A. V.; Stathis, P.; Permuth, S. F.; Tokes, L.; Feldman, D. Bisphenol-A: an estrogenic substance is released from polycarbonate flasks during autoclaving. *Endocrinology* **1993**, *132* (6), 2279–2286.

(56) Staples, C. A.; Dome, P. B.; Klecka, G. M.; Oblock, S. T.; Harris, L. R. A review of the environmental fate, effects, and exposures of bisphenol A. *Chemosphere* **1998**, *36* (10), 2149–2173.

(57) Dann, A. B.; Hontela, A. Triclosan: environmental exposure, toxicity and mechanisms of action. *J. Appl. Toxicol. JAT* **2011**, *31* (4), 285–311.

(58) Barron, M. *Toxicological review of phenol in support of summary information on Integrated Risk Information System (IRIS).*; U.S. Environmental Protection Agency: Washington DC, 2002.

(59) Gross, K. C.; Seybold, P. G. Substituent effects on the physical properties and pKa of phenol. *Int. J. Quantum Chem.* **2001**, *85* (4-5), 569–579.

(60) Ukrainczyk, L.; McBride, M. B. The oxidative dechlorination reaction of 2,4,6-trichlorophenol in dilute aqueous suspensions of manganese oxides. *ETC Environ. Toxicol. Chem.* **1993**, *12* (11), 2005–2014.

(61) Sangster, J. *Octanol-Water Partition Coefficients: Fundamentals and Physical Chemistry*; John Wiley & Sons, 1997.

(62) Mackay, D. *Illustrated handbook of physical-chemical properties and environmental fate for organic chemicals*; Boca Raton : Boca Raton :, 1992.

(63) Cousins, I. T.; Staples, C. A.; Klecka, G. M.; Mackay, D. A Multimedia Assessment of the Environmental Fate of Bisphenol A. *Hum. Ecol. Risk Assess. Int. J.* **2002**, *8* (5), 1107–1135.

(64) Clara, M.; Strenn, B.; Saracevic, E.; Kreuzinger, N. Adsorption of bisphenol-A, 17β-estradiole and 17α-ethinylestradiole to sewage sludge. *Chemosphere* **2004**, *56* (9), 843–851.

(65) Li, H.; Lee, L. S.; Schulze, D. G.; Guest, C. A. Role of soil manganese in the oxidation of aromatic amines. *Environ. Sci. Technol.* **2003**, *37* (12), 2686–2693.

(66) Reiss, R.; Mackay, N.; Habig, C.; Griffin, J. An ecological risk assessment for triclosan in lotic systems following discharge from wastewater treatment plants in the United States. *Environ. Toxicol. Chem.* **2002**, *21* (11), 2483–2492.

(67) Lin, K.; Liu, W.; Gan, J. Oxidative Removal of Bisphenol A by Manganese Dioxide: Efficacy, Products, and Pathways. *Environ. Sci. Technol.* **2009**, *43*, 3860.

(68) Desbrow, C.; Routledge, E. J.; Brighty, G. C.; Sumpter, J. P.; Waldock, M. Identification of Estrogenic Chemicals in STW Effluent. 1. Chemical Fractionation and in Vitro Biological Screening. *Environ. Sci. Technol.* **1998**, *32* (11), 1549–1558.

(69) Routledge, E. J.; Sheahan, D.; Desbrow, C.; Brighty, G. C.; Waldock, M.; Sumpter, J. P. Identification of Estrogenic Chemicals in STW Effluent. 2. In Vivo Responses in Trout and Roach. *Environ. Sci. Technol.* **1998**, *32* (11), 1559–1565.

(70) Mawhinney, D. B.; Young, R. B.; Vanderford, B. J.; Borch, T.; Snyder, S. A. Artificial Sweetener Sucralose in U.S. Drinking Water Systems. *Environ. Sci. Technol.* **2011**, *45* (20), 8716–8722.

(71) Buerge, I. J.; Buser, H.-R.; Kahle, M.; Müller, M. D.; Poiger, T. Ubiquitous Occurrence of the Artificial Sweetener Acesulfame in the Aquatic Environment: An Ideal Chemical Marker of Domestic Wastewater in Groundwater. *Environ. Sci. Technol.* **2009**, *43* (12), 4381–4385.

(72) Buerge, I. J.; Poiger, T.; Müller, M. D.; Buser, H.-R. Caffeine, an Anthropogenic Marker for Wastewater Contamination of Surface Waters. *Environ. Sci. Technol.* **2003**, *37* (4), 691–700.

(73) Luo, Y.; Guo, W.; Ngo, H. H.; Nghiem, L. D.; Hai, F. I.; Zhang, J.; Liang, S.; Wang, X. C. A review on the occurrence of micropollutants in the aquatic environment and their fate and removal during wastewater treatment. *Sci. Total Environ.* **2014**, *473–474*, 619–641.

(74) Knocke, W. R.; Hoehn, R. C.; Sinsabaugh, R. L. Using Alternative Oxidants to Remove Dissolved Manganese From Waters Laden With Organics. *J. Am. Water Works Assoc.* **1987**, *79* (3), 75–79.

(75) Morgan, J. J.; Stumm, W. Analytical Chemistry of Aqueous Manganese. *J. Am. Water Works Assoc.* **1965**, *57* (1), 107–119.

(76) Stone, A. T.; Ulrich, H.-J. Kinetics and reaction stoichiometry in the reductive dissolution of manganese(IV) dioxide and co(III) oxide by hydroquinone. *J. Colloid Interface Sci.* **1989**, *132* (2), 509–522.

(77) Selig, H.; Keinath, T. M.; Weber, W. J. Sorption and Manganese-Induced Oxidative Coupling of Hydroxylated Aromatic Compounds by Natural Geosorbents. *Environ. Sci. Technol.* **2003**, *37* (18), 4122–4127.

(78) Banerjee, D.; Nesbitt, H. W. XPS study of reductive dissolution of birnessite by oxalate: rates and mechanistic aspects of dissolution and redox processes. *Geochim. Cosmochim. Acta* **1999**, *63* (19–20), 3025–3038.

(79) Taujale, S.; Zhang, H. Impact of Interactions between Metal Oxides to Oxidative Reactivity of Manganese Dioxide. *Environ. Sci. Technol.* **2012**, *46* (5), 2764–2771.

(80) Ding, J.; Su, M.; Wu, C.; Lin, K. Transformation of triclosan to 2,8-dichlorodibenzo-p-dioxin by iron and manganese oxides under near dry conditions. *Chemosphere* **2015**, *133*, 41–46.

(81) Lu, Z.; Lin, K.; Gan, J. Oxidation of bisphenol F (BPF) by manganese dioxide. *Environ. Pollut. Barking Essex 1987* **2011**, *159*, 2546–2551.

(82) Zhang, H.; Huang, C.-H. Adsorption and oxidation of fluoroquinolone antibacterial agents and structurally related amines with goethite. *Chemosphere* **2007**, *66* (8), 1502–1512.

(83) Cerrato, J. M.; Hochella, M. F.; Knocke, W. R.; Dietrich, A. M.; Cromer, T. F. Use of XPS to Identify the Oxidation State of Mn in Solid Surfaces of Filtration Media Oxide Samples from Drinking Water Treatment Plants. *Environ. Sci. Technol.* **2010**, *44*, 5881–5886.

(84) Jodi L. Junta, M. F. H. Manganese (II) oxidation at mineral surfaces: A microscopic and spectroscopic study. *Geochim. Cosmochim. Acta* **1994**, *58* (22), 4985–4999.

69

(85) Ilton, E. S.; Post, J. E.; Heaney, P. J.; Ling, F. T.; Kerisit, S. N. XPS determination of Mn oxidation states in Mn (hydr)oxides. *Appl. Surf. Sci.* **2016**, *366*, 475–485.

(86) Briggs, D.; Beamson, G. XPS studies of the oxygen 1s and 2s levels in a wide range of functional polymers. *Anal. Chem.* **1993**, *65* (11), 1517–1523.

(87) Briggs, D.; Beamson, G. Primary and secondary oxygen-induced C1s binding energy shifts in x-ray photoelectron spectroscopy of polymers. *Anal. Chem.* **1992**, *64* (15), 1729–1736.

(88) Busetti, F.; Backe, W. J.; Bendixen, N.; Maier, U.; Place, B.; Giger, W.; Field, J. A. Trace analysis of environmental matrices by large-volume injection and liquid chromatography–mass spectrometry. *Anal. Bioanal. Chem.* **2011**, *402* (1), 175–186.

(89) Backe, W. J.; Ort, C.; Brewer, A. J.; Field, J. A. Analysis of Androgenic Steroids in Environmental Waters by Large-Volume Injection Liquid Chromatography Tandem Mass Spectrometry. *Anal. Chem.* **2011**, *83* (7), 2622–2630.

(90) Busetti, F.; Backe, W. J.; Bendixen, N.; Maier, U.; Place, B.; Giger, W.; Field, J. A. Trace analysis of environmental matrices by large-volume injection and liquid chromatography–mass spectrometry. *Anal. Bioanal. Chem.* **2011**, *402* (1), 175–186.

(91) Colborn, T.; Frederick, S. vom S.; Soto, A. M. Developmental Effects of Endocrine-Disrupting Chemicals in Wildlife and Humans. *Envihealpers Environ. Health Perspect.* **1993**, *101*, 378–384.

(92) Yamasaki, K.; Takeyoshi, M.; Yakabe, Y.; Sawaki, M.; Imatanaka, N.; Takatsuki, M. Comparison of reporter gene assay and immature rat uterotrophic assay of twenty-three chemicals. *Toxicology* **2002**, *170* (1–2), 21–30.

(93) Rule, K. L.; Ebbett, V. R.; Vikesland, P. J. Formation of Chloroform and Chlorinated Organics by Free-Chlorine-Mediated Oxidation of Triclosan. *Environ. Sci. Technol.* **2005**, *39* (9), 3176–3185.

(94) Levy, S. B. Antibacterial household products: cause for concern. *Emerg. Infect. Dis.* **2001**, *7* (3 Suppl), 512–515.

(95) McMurry, L. M.; Oethinger, M.; Levy, S. B. Triclosan targets lipid synthesis. *Nature* **1998**, *394* (6693), 531–532.

(96) Latch, D. E.; Packer, J. L.; Arnold, W. A.; McNeill, K. Photochemical conversion of triclosan to 2, 8-dichlorodibenzo-p-dioxin in aqueous solution. *J. Photochem. Photobiol. Chem.* **2003**, *158*, 63–66.

(97) Stone, A. T.; Morgan, J. J. Reduction and dissolution of manganese(III) and manganese(IV) oxides by organics. 1. Reaction with hydroquinone. *Environ. Sci. Technol.* **1984**, *18* (6), 450–456.

(98) Stone, A. T.; Morgan, J. J. Reduction and dissolution of manganese(III) and manganese(IV) oxides by organics: 2. Survey of the reactivity of organics. *Environ. Sci. Technol.* **1984**, *18* (8), 617–624.

(99) Rudder, J. de; Wiele, T. V. de; Dhooge, W.; Comhaire, F.; Verstraete, W. Advanced water treatment with manganese oxide for the removal of 17a-ethynylestradiol (EE2). *WR Water Res.* **2004**, *38*, 184–192.

(100) Geszvain, K.; Butterfield, C.; Davis, R. E.; Madison, A. S.; Lee, S.-W.; Parker, D. L.; Soldatova, A.; Spiro, T. G.; Luther, G. W.; Tebo, B. M. The molecular biogeochemistry of manganese(II) oxidation. *Biochem. Soc. Trans.* **2012**, *40* (6), 1244–1248.

(101) Beamson, G.; Briggs, D.; SurfaceSpectra Ltd. *The XPS of polymers database.*; SurfaceSpectra,: Manchester, 2000.

70

(102) Ching, S.; Petrovay, D. J.; Jorgensen, M. L.; Suib, S. L. Sol–Gel Synthesis of Layered Birnessite-Type Manganese Oxides. *Inorg. Chem.* **1997**, *36* (5), 883–890.

(103) Armstrong, F. A. Why did Nature choose manganese to make oxygen? *Philos. Trans. R. Soc. Lond. B Biol. Sci.* **2008**, *363* (1494), 1263–1270.

(104) Kitamura, S.; Suzuki, T.; Sanoh, S.; Kohta, R.; Jinno, N.; Sugihara, K.; Yoshihara, S. 'ichi; Fujimoto, N.; Watanabe, H.; Ohta, S. Comparative Study of the Endocrine-Disrupting Activity of Bisphenol A and 19 Related Compounds. *Toxicol. Sci.* **2005**, *84* (2), 249–259.

71